CHALMERS
UNIVERSITY OF TECHNOLOGY

The function of key microbial guilds in full-scale wastewater treatment reactors with aerobic granular sludge

Master's Thesis in Infrastructure and Environmental Engineering

VASANTH RAMESH

Department of Architecture and Civil Engineering
Division of Water Environment Technology
CHALMERS UNIVERSITY OF TECHNOLOGY
Master's Thesis ACEX60
Gothenburg, Sweden 2020

CHALMERS
UNIVERSITY OF TECHNOLOGY

Department of Architecture and Civil Engineering
Division of Water Environment Technology
CHALMERS UNIVERSITY OF TECHNOLOGY
Master's Thesis ACEX60
Gothenburg, Sweden 2020

MASTER'S THESIS ACEX60

The function of key microbial guilds in full-scale wastewater treatment reactors with aerobic granular sludge

Master's Thesis in the master's Programme Infrastructure and Environmental Engineering

VASANTH RAMESH

Department of Architecture and Civil Engineering
Division of Water Environment Technology

CHALMERS UNIVERSITY OF TECHNOLOGY
Göteborg, Sweden 2020

The function of key microbial guilds in full-scale wastewater treatment reactors with aerobic granular sludge

Master's Thesis in the Master's Programme Infrastructure and Environmental Engineering

VASANTH RAMESH

Examensarbete ACEX60 / Institutionen för bygg- och miljöteknik, Chalmers tekniska högskola 2020

Department of Architecture and Civil Engineering
Division of Water Environment Technology

CHALMERS UNIVERSITY OF TECHNOLOGY
SE-412 96 Göteborg
Sweden
Telephone: + 46 (0)31-772 1000

Cover:
Experiment set-up in which batch activity tests were performed

Master's thesis in the Master's Programme Infrastructure and Environmental Engineering

VASANTH RAMESH
Department of Architecture and Civil Engineering
Division of Water Environment Technology
CHALMERS UNIVERSITY OF TECHNOLOGY

ABSTRACT

Aerobic Granular Sludge (AGS) is aggregated microbial growth in the form of granules. The use of AGS technology in wastewater treatment operations can significantly reduce land footprint, energy, and chemical consumption. The goal of the thesis was to study the performance of these aggregates under controlled environmental conditions. Batch activity tests were carried out to study the nitrification, denitrification, and polyphosphate accumulation process in mixed granules (a mixture of all granule sizes) and sieved granules (different granule sizes). It has been observed that performing experiments at relatively high sludge concentrations (15 g/L), and at pH 7.5±0.1, can provide favourable environmental conditions to study the PAO activity in terms of high P-release and P-released to acetate consumed ratio (P-release/C up-take). The PAO activity rate seems to be higher in relatively larger granules (>2mm) while nitrogen removal performance i.e. nitrification and denitrification appears to be more efficient in smaller granules (<2mm). The low P-release/C up-take during the anaerobic phase suggests presence and, in some cases, the dominance of GAO metabolism irrespective of granule sizes. DPAO activity seems to be suppressed or even absent in both the granule sizes. The strong correlation (>0.95) between co-release of cations and PO_4^{3-}-P during the anaerobic phase suggests the breakage of poly-P reserves in PAOs to take up acetate from the solution.

Keywords:
Aerobic Granular Sludge, batch activity tests, nitrogen and phosphorous removal, granule sizes

Acknowledgements

First, I like to thank Jennifer, my supervisor for tolerating, and helping me throughout this work. Special thanks to Cecilia and Amir, for shaping my Chalmers days memorable, enriching, and as well as for making the WET lab my second home. Frank for giving me the opportunity and making wastewater course a joyful one. Britt-Marie for the valuable insights during the thesis and making this report readable. Oskar for helping me with HPLC and I always admired his vast expertise in the subject. Thanks to all the Ph.D. students in WET especially Marie, Mohanna, Victor, Anna, Nashita for the nice conversations. David, Tim, and Mark for giving their perspectives during the work. Thanks to my lab colleagues Rose and Celia.

“Everything is everywhere but the environment selects”
- Baas Becking, 1934.

List of abbreviations

Abbreviation	Full description
ADP	Adenosine di-phosphate
AGS	Aerobic granular sludge
AND	Alternating nitrification-denitrification
AOB	Ammonium oxidizing bacteria
AP	Apatite phosphorous
ATP	Adenosine triphosphate
COD	Chemical oxygen demand
DO	Dissolved oxygen
DPAO	Denitrifying phosphate accumulating organisms
EBPR	Enhanced biological phosphorous removal
EPS	Extracellular polymeric substance
GAO	Glycogen accumulating organisms
HRT	Hydraulic retention time
IC	Ion chromatography
IP	Inorganic phosphorous
MBR	Membrane bio-reactor
MLSS	Mixed liquor suspended solids
MLVSS	Mixed liquor volatile suspended solids
NAD	Nicotinamide adenine dinucleotide
NAIP	Non-apatite inorganic phosphorus
NOB	Nitrite oxidizing bacteria
OP	Organic phosphorous
OHO	Ordinary heterotrophic organisms
PAO	Phosphate accumulating organisms
PHA	Poly-hydroxy-alkanoates
PHB	Poly-hydroxy-butyrate
PP	Polyphosphate
SBR	Sequencing batch reactor
SND	Simultaneous nitrification-denitrification
SNDP	Simultaneous nitrification-denitrification and phosphorous removal
SRT	Solids retention time
SVI	Sludge volume index
TCA	Tricarboxylic acid cycle
TP	Total phosphorous
UASB	Upflow anaerobic sludge blanket
VFA	Volatile Fatty acids
VSS	Volatile suspended solids
WWTP	Wastewater treatment plant

LIST OF FIGURES

Figure 1. Ion translocation in anaerobic conditions across the cytoplasmic membrane (Wentzel, et al., 1986) 9
Figure 2. Ion translocation in aerobic conditions across the cytoplasmic membrane (Wentzel et al., 1986) 10
Figure 3. Schematic diagram illustrating the EBPR process in an activated sludge treatment plant (van Loosdrecht et al., 2016). 11
Figure 4. A typical aerobic granular structure. 13
Figure 5. Experimental setup. 22
Figure 6. Sludge washing steps. 24
Figure 7. Steps in sludge preparation. a) the sludge after transfer from the container. b) the sludge from step a) is diluted again with synthetic wastewater to achieve the desired concentration. 25
Figure 8. Sampling method. 27
Figure 9. The parameters (environmental conditions) that were controlled and monitored during the test: temperature, carbon source, and the parameters that were varied during the test are listed. Tests were performed with mixed and sieved granules at controlled environmental conditions and by changing the variable parameters to study its influence on granules performance. 32
Figure 10. a, b, c and d show the trend of anaerobic $PO4^{3-}$-P release and COD uptake during the anaerobic period at measured influent COD/P ratio 3, 10, 30 and 9 respectively. 37
Figure 11. a, b, c, d, e, f, g and h show the trend of anaerobic $PO4^{3-}$-P release and COD uptake during the anaerobic period of mixed sludge maintained at different MLSS concentrations 39
Figure 12. a, b, c, d, e, f, g, and h show the trend of anaerobic $PO4^{3-}$-P release and COD uptake during the anaerobic period of sieved granules maintained at different MLSS concentrations. 42
Figure 13. a, b, c, and d show the trend of anaerobic $PO4^{3-}$-P release and COD uptake during the anaerobic period of mixed granules maintained at different pH. 44
Figure 14. a and b illustrate the trend of $PO4^{3-}$-P release and uptake in test mixed granules respectively. 45
Figure 15. a) sludge samples were taken out from WWTP during aeration phase b) sludge transport in icebox (anaerobic conditions) c) stored in the refrigerator for about 16 hours (anaerobic conditions) d) sludge washing (aerobic conditions) before the test. 46
Figure 16. a and b illustrate the trend of $NH4^{+}$-N, $PO4^{3-}$-P uptake and $NO3^{-}$-N production during nitrification in mixed granules. 47
Figure 17. a and b illustrate the trend of $NO3^{-}$-N uptake, acetate uptake and $PO4^{3-}$-P release during denitrification in mixed granules. 49
Figure 18. a, b, c, d, e, and f illustrate the trend of $PO4^{3-}$-P ions and COD concentration in the bulk liquid during the tests with different granule sizes < 2mm, > 2mm. 50
Figure 19. a and b illustrate the trend of $NH4^{+}$-N, $PO4^{3-}$-P uptake and $NO3^{-}$-N production during nitrification in granule sizes > 2mm, <2mm respectively. 51
Figure 20. a and b illustrate the trend of $NO3^{-}$-N uptake, acetate uptake during denitrification in granule sizes > 2mm, <2mm respectively. 52

Figure 21. Coefficient (slope) for expected and observed concentrations for all the standard ions 60
Figure 22. a, b, c, and d illustrate the cations and P release during anaerobic phase in test 21, 22, 23, and 24 respectively. 64

Contents

1 Introduction 1

1.1 Background 1
1.1.1 Wastewater treatment - Journey through the years 1
1.1.2 Sequencing Batch Reactor 1
1.1.3 A paradigm of compact WWTP 3

1.2 Aim 5

1.3 Objectives 5

1.4 Limitations 5

2 Literature Review 6

2.1 Nitrogen removal 6
2.1.1 Nitrification 6
2.1.2 Denitrification 6

2.2 Bio-P Removal 7
2.2.1 Anaerobic phase 8
2.2.2 Aerobic phase 9
2.2.3 PAO, GAOs, and EBPR 11

2.3 AGS - an overview 12
2.3.1 Granule structure & size 12
2.3.2 Density 15
2.3.3 Settling Velocity 15
2.3.4 SVI 16
2.3.5 External mass transfer limitations 16
2.3.6 Carbon leakage 17
2.3.7 Dissolved Oxygen 18
2.3.8 Granule Porosity 18

2.4 Batch activity tests 19

3 Materials and methods 20

3.1 Synthetic wastewater composition 20

3.2 Experiment procedure 21
3.2.1 Reactor setup 21
3.2.2 Bio-P activity test 22
3.2.3 Nitrification test & denitrification activity test 23

3.3 Sludge washing 23
3.3.1 Initial method 23
3.3.2 Sludge washing-Final method 25

3.4 pH Control 26

3.5 Sample preparation for IC 26

3.6 Analyzing the samples in IC 27

3.7 Adding external carbon and phosphate source 28

3.8 MLSS and MLVSS test 29
3.9 Kinetic and stoichiometric parameters estimation 30
3.10 Experiment set-up 31
3.10.1 Effect of influent COD/P on anaerobic PO_4^{3-}-P release kinetics 32
3.10.2 Effect of MLSS on anaerobic PO_4^{3-}-P release kinetics 33
3.10.3 Batch activity test with mixed granules 33
3.10.4 Effect of pH 34
3.10.5 Effect of Granule size 34
3.10.6 Bio-P activity in sieved granules 34
3.10.7 Nitrification & denitrification in sieved granules 35
3.11 Uncertainties and error sources 35

4 Results and discussions 36
4.1 Effect of influent COD/P on anaerobic PO_4^{3-}-P release kinetics 36
4.2 Effect of MLSS on anaerobic PO_4^{3-}-P release kinetics 38
4.2.1 The effect in mixed granules 38
4.2.2 The effect in sieved granules 40
4.3 Effect of pH on anaerobic PO_4^{3-}-P release kinetics 43
4.4 Batch activity test with mixed sludge 45
4.4.1 Bio-P activity test 45
4.4.2 Nitrification and denitrification activity test 46
4.5 Effect of granule size 49
4.5.1 Bio- P activity 49
4.5.2 Nitrification in sieved granules 51
4.5.3 Denitrification in sieved granules 52

5 Conclusions 53

REFERENCES 55

APPENDIX-A 58

APPENDIX-B 59

APPENDIX-C 60

APPENDIX-D 61

APPENDIX-E 63

APPENDIX-F 64

1 Introduction

In this chapter, a brief background to the development of wastewater treatment from the Roman era until today is presented.

1.1 Background

1.1.1 Wastewater treatment - Journey through the years

The remarkable underground sanitation system, that networks the city of Rome to carry the generated wastewater to river Tiber is an engineering marvel. The knowledge had been passed from the Greek's understanding of the relationship between water quality and public health which was passed to the Roman Empire (De Kreuk et al., 2006).

The treatment plants built before world war II had only mechanical separation and settling without biological treatment. The breakthrough discovery of activated sludge by Arden and Lockett paved the development of a new era of wastewater treatment with suspended growth treatment in the 1920s. The two types of configuration 1) continuous flow 2) batch flow (fill-and-draw arrangement) were tested from the earliest times of activated sludge treatment. Activated sludge systems remain the most widely used treatment process for wastewater treatment even today. The mixture of different microbial guilds in the biomass sludge enables the efficient removal of organic carbon and nutrients. The growth of photosynthetic microorganisms like algae and cyanobacteria depends on the availability of phosphorous. Phosphorous is a key nutrient that simulates eutrophication in water bodies must be removed from wastewater for safe disposal (Oehmen et al., 2007). The main process of these systems is the biochemical reactions in the aerated/non-aerated bioreactors followed by separation in secondary clarifiers as the follow-up step. The strategic selection of key microbial guilds that can metabolize the polluting agents followed by efficient separation of water, air, and biomass in settling tanks after the treatment influences the efficient performance of these systems

1.1.2 Sequencing Batch Reactor

The steps in a Sequencing Batch Reactor (SBR) include fill, react, settling, draw, and idle. SBR process works in a fill-and-draw mode where aeration, sedimentation/clarification occurs in the same tank in subsequent time steps.

The cycle length in SBR treatment can range from a few hours to the entire day. Although SBR is fed discontinuously, conventional continuous flow operations as that of activated sludge systems, contact stabilization, etc., can be achieved by running parallel reactors (De Kreuk et al., 2006). Operating two or more SBRs enables continuous flow operation, as one tank is filled, other reactors would be at the subsequent phases of the treatment process. Biological nitrogen and phosphorus removal can be achieved by changing the aerobic/anaerobic phases in the treatment cycle (Metcalf and Eddy, 2014).

Steps in an SBR treatment process

1. Fill – The fill operation typically involves increasing the volume of the reactor and includes the addition of the substrate. Mixed with stirrer alone, aeration coupled with mixing are possible configurations during this step depending on the biological treatment to be carried out.
2. React – Under controlled environmental conditions, the substrates are degraded by the biomass in the reactor.
3. Settle – During the settling operation, the biomass and the treated water is separated by gravity settling. The separated supernatant is discharged as effluent.
4. Decant – The decant operation involves the separation of the treated effluent by using decanting mechanisms like floating or adjustable weirs.
5. Idle – Idle phase in an SBR process can be omitted. In the SBR treatment process with multiple tanks, when one reactor is under fill operation another reactor can be in the idle phase before switching to another tank.

Ardern's rationale to go for continuous flow systems instead of batch arrangement (today's Sequencing Batch Reactor) was due to the reasons below:

1. Operation ease with continuous flow in the switching of valves and cleaning of diffusers.
2. To prevent clogging of coarse bubble diffusers that were used at that time.

The SBR (Sequencing Batch Reactor) came back to the picture after the work of Hoover in the 1940s and Pasveer in the 1960s. Even now, continuous flow configurations are the most prevalent, with SBR being used mainly for industrial and small WWTPs (Metcalf and Eddy, 2014).

1.1.3 A paradigm of compact WWTP

Conventional wastewater treatment has a very large footprint in terms of both land space required and energy. To cope with the ever-increasing population and urban agglomeration, it is necessary to investigate alternative compact wastewater treatment systems. The chapter briefly introduces the readers to compact treatment systems that are getting more attention.

1.1.3.1 Anaerobic granules

High loading rates in the range of 40 kg COD m^{-3} day^{-1} has been possible by employing anaerobic granules (De Kreuk et al., 2006). Compact treatment systems in which the biomass can be effectively retained because of its high settleability has been followed in anaerobic systems for the last three decades. Methane generation by methanogenic microbes enables energy generation. Anaerobic treatment can handle high organic carbon loading, for instance, septic tank sludge, but its low nutrient removal efficiency prevents its widespread usage, as additional treatment steps are required. Operation at higher temperatures (>20^{o}C) and its low growth yield if good inoculum or seed sludge is not available, which leads to very long start-up time are also other major concerns.

1.1.3.2 Membrane Bio-reactors

The Membrane Bio-reactors (MBR) are systems in which the activated sludge is combined with a membrane, for instance, microfilter or ultrafilter membrane in a single unit (De Kreuk et al., 2006). The compactness achieved using membrane allows conversion of the existing secondary clarifiers or aeration tanks into MBR units without the need for reconstruction. The removal of bacteria and viruses is higher than conventional activated sludge systems with superior effluent quality achieved by efficient removal of colloids and suspended particles. Higher sludge concentration is possible than in conventional systems within a relatively smaller space.

The overall nitrogen removal can be better in MBRs as the solids retention time (SRT) of the slow-growing organisms is significantly higher than conventional activated sludge systems. By introducing anaerobic chambers/units physically or having an anaerobic phase in the treatment cycle, denitrification can be achieved efficiently. The problems by using the MBR process includes frequent membrane fouling due to high sludge concentration and the relatively high energy consumption.

1.1.3.3 Biofilm reactors

Even while maintaining short hydraulic retention times, biofilm reactors are effective in retaining slow-growing autotrophs (De Kreuk et al., 2006). Two possible configurations of the biofilm reactor system are static biofilm reactor, for instance, trickling filter or reactor with a suspended carrier i.e. particle supported biofilms; mostly plastic carriers nowadays. The specific surface area of particle suspended carriers can be significantly high in the range of 3000 m^2 m^{-3}, hence high biomass concentration is possible when compared to its static biofilm counterparts with the specific surface area of only 300 m^2 m^{-3}. Compact reactor design has been achieved due to the efficient retainment of biomass in the reactor, eliminating the need for external clarifiers. The competition for limited space between heterotrophs and autotrophs, the requirement of complex construction for separation of effluent from biomass are some of the major limitations with these systems.

1.1.3.4 AGS and SBR

The secondary settling tanks have been the bottleneck of biological treatment, as the maximum hydraulic load it can handle is low (De Kreuk et al., 2006). The low hydraulic loading is a result of low settling velocities of the conventional activated sludge. The space required for these traditional technologies is relatively high and with increasing urban agglomeration, the need for new compact systems has been a central part of the discussion. The requirement of huge sedimentation tanks and comparatively low sludge concentrations in the bioreactor makes the conventional wastewater treatment plants uneconomical in terms of large land and energy footprints. The large hydraulic loadings in a domestic WWTP coupled with the necessity to separate the water, air and biomass phase of the wastewater constituent makes the conventional system quite complicated.

The technologies that have been developed during the last decades have been relatively compact with potential advantages compared to conventional activated sludge systems. The use of Aerobic Granular Sludge (AGS) in combination with SBR enables a significant reduction in the land space required and makes the treatment system more compact. In the SBR process, the process of settling takes place in the same reactor and the separation of water and biomass is rather temporal instead of being spatial as in the case of conventional activated sludge plant, therefore saving the need for using complex and expensive internal settling chambers.

1.2 Aim

The thesis aims to study the function of key microbial guilds with aerobic granular sludge and the factors that underpin the variation in their activity by applying batch activity tests.

1.3 Objectives

The specific objectives that the thesis focuses are to:

1. Develop a method to perform biological phosphorus uptake and release, nitrification, and denitrification batch activity tests with aerobic granules.
2. Assess the reproducibility of the activity tests to be able to use them as input to future operations of full-scale AGS wastewater treatment plants (WWTPs).
3. Assess the activity of bacterial guilds based on aggregate size by applying activity tests on mixed and sieved aerobic granules.
4. Study the temporal variation in the activity of the key microbial guilds at a full-scale AGS WWTP.

1.4 Limitations

- The microbial composition of the aggregates was not analyzed in this work.
- Real wastewater was not used for the experiments.
- Acetate was the only carbon source available for microbial activity.
- Sludge taken from the wastewater treatment plant was stored in the refrigerator and it was later used for experiments (within 24 hours).
- Objectives 4 was not focussed due to time limitations especially due to the COVID-19 crisis.

2 Literature Review

The chapter discusses the underlying theory behind the biological nitrogen and phosphorous removal process in wastewater treatment and attempts to give a perspective of recent developments in AGS. A short note on batch activity tests is also presented.

2.1 Nitrogen removal

2.1.1 Nitrification

Nitrification is a two-step process involving the conversion of ammonium to nitrite followed by nitrite to nitrate conversion, the conversion process is carried out by ammonium oxidizing bacteria (AOB), nitrite-oxidizing bacteria (NOB) respectively. Nitrification is a natural process that occurs in soil, rivers, lakes to the nitrifying organisms given that an enabling environment is provided (Henze, 1995). The slow growth rate of nitrifying organisms is due to the low energy yield by oxidation of ammonium and nitrite for AOB and NOB respectively.

$$NH_4^+ + 1.5O_2 \longrightarrow NO_2^- + H_2O + 2H^+ \quad \text{.....[1]}$$

$$NO_2^-\text{-}N + 0.5O_2 \longrightarrow NO_3^- \quad \text{.....[2]}$$

The reaction involves the reduction in the pH of the system as 2 moles of protons are released per mole of ammonium oxidized (van Loosdrecht et al., 2016). The carbonates (alkalinity) available in the domestic wastewater buffers the pH but the pH might fall below 7.0 under insufficient conditions. About 1.8 % of the ammonium taken up for nitrification is utilized for cell assimilation.

2.1.2 Denitrification

Denitrifying guilds are generally facultative heterotrophic organisms that convert nitrate into nitrogen gas in the presence of a carbon source (Henze, 1995). The nitrate acts as an electron acceptor while the carbon source acts as an electron donor. The intermediary products of denitrification are shown in equation 3 and they are also toxic greenhouse gases.

$$NO_3^- \longrightarrow NO_2^- \longrightarrow NO \longrightarrow N_2O \longrightarrow N_2 \quad \text{..... [3]}$$

The alkalinity of the system is increased, as 1 mole of alkalinity is generated per mole of nitrate conversion in denitrification. The factors influencing denitrification reaction are carbon substrate availability (denitrifying guilds can use a wide spectrum of the substrate), pH, temperature, oxygen as it inhibits the process.

2.2 Bio-P removal

The efficiency of biological phosphorus removal in wastewater treatment plants lies in the tendency of phosphorous accumulating organisms (PAOs) (e.g. Acinetobacter) to accumulate excess phosphorous than required for metabolism and natural precipitation (Oldham, 1986). In mixed cultures under aerobic conditions, the PAOs are outcompeted by other heterotrophs for substrate and hence it's hard to sustain growth. In case of the availability of Volatile Fatty Acids (VFAs) under anaerobic conditions, the PAOs can take up these VFAs, as there is no competition from other heterotrophs due to the absence of electron acceptor. The bond energy released from breaking down the stored polyphosphate chain is used as an energy source for sequestering the carbon substrate. The concentration of phosphate in the surrounding liquid is increased as a result of this process. When the PAOs are exposed from anaerobic zone to a zone with the presence of oxygen, the stored carbon source is used for two purposes 1) for taking up PO_4^{3-}-P from the surrounding medium 2) growth. This exclusive way of sequestering carbon substrate during anaerobic conditions and its utilization during aerobic conditions provides a competitive advantage over other heterotrophs to sustain its growth.

The presence of VFAs in domestic wastewater is generally too low, to expect any phosphorous uptake or release (Dold, and Ekama, 1985). It has been observed that biological phosphorous removal has a strong dependency on the presence of readily biodegradable COD (complex soluble COD) in the influent. The hydrolysis process is as follows: The non-poly P organisms take up the readily biodegradable carbon fraction from the wastewater during anaerobic conditions and breaks down to VFAs using the glycolytic (Embden-Meyerhof) pathway. The breakdown products (VFAs) are released into the surrounding medium which is sequestered by the poly-P organisms. Thus, the activity of non-poly P organisms (facultative aerobes) influences biological phosphorus removal at low influent VFAs availability. The presence of an electron acceptor (e.g. NO_3^--N) in the anaerobic zone adversely affects the biological phosphorous release. The non-poly P organisms can utilize the carbon substrate using an oxidative process

(citric acid cycle for instance) and thus no useful VFA product is produced that can be sequestered by the poly-P organisms.

2.2.1 Anaerobic phase

The anaerobic phase is characterized by the absence of an electron acceptor but with the availability of readily biodegradable carbon substrate (Wentzel et al., 1986). The absence of an electron acceptor increases the NADH/NAD ratio which inhibits the ATP generation and hence decreases the ATP/ADP ratio. "The effect of these changes in NADH/NAD ratio and ATP/ADP ratio inhibits and simulates the Tricarboxylic acid cycle (TCA) respectively". ATP production stimulated by the decrease in ATP/ADP ratio, in turn, stimulates the breakdown of stored polyphosphate chain (by hydrolysis) and the high energy phosphoryl group is transferred to ADP. The TCA cycle is made possible under the availability of an electron sink to NADH (decreases NADH/NAD ratio). The substrate nature defines the source of electrons. If both carbon and energy source is available, and the NADH/NAD and ATP/ADP ratio are high enough, then the carbon substrate is stored as PHB. In the case of acetate being the carbon substrate, the fate of the substrate can be summarized as follows:

1) The high concentration of the acetate in the liquid medium allows the passive diffusion of the molecule into the cytoplasmic cell membrane by passive diffusion without any energy consumption/requirement.
2) The conversion of acetate into acetyl-CoA decreases the ATP, thus a decrease in ATP/ADP ratio. The decrease in ATP/ADP ratio simulates the breakdown of the polyphosphate chain (by hydrolysis) to produce ATP. The free phosphate concentration and cations that have helped stabilize the poly-P are also increased within the cell. The cations and phosphate are released into the surrounding liquid medium. The outline of the translocation of ions in the anaerobic phase is depicted in Figure 2.
3) PHB production is thus simulated by the high concentration of acetyl-CoA and associated high NADH/NAD ratio. The reduction of acetoacetyl-CoA to β-hydroxybutyryl-CoA takes place with the oxidation of NADH to NAD during the formation of PHB. Thus, the inhibition on the TCA cycle is removed, as PHB synthesis acts as an electron sink by decreasing the NADH/NAD ratio. The decrease in NADH/NAD ratio simulates the TCA cycle and associated

glyoxylate cycle, resulting in electron generation and thereby an increase in the NADH/NAD ratio. The biochemical regulation mediated by NADH/NAD on the TCA cycle and PHB synthesis help in ensuring the availability of protons and electrons for storing acetate as PHB. An elaborate text on the phenomenon can be accessed by the reader elsewhere.

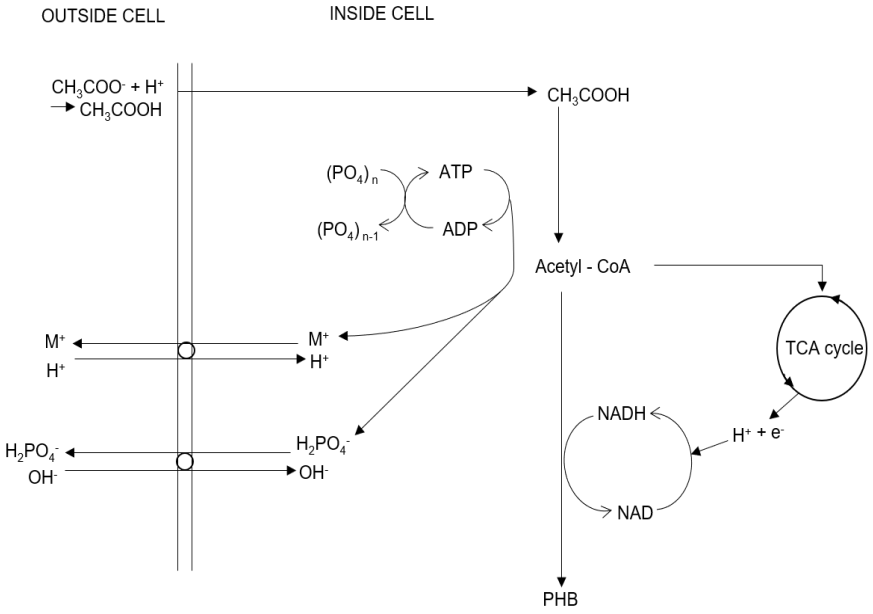

Figure 1. Ion translocation in anaerobic conditions across the cytoplasmic membrane (Wentzel, et al., 1986)

2.2.2 Aerobic phase

The aerobic phase can be characterized by the low availability of a readily biodegradable substrate (limited availability) but with the presence of an electron acceptor and PHB stored from the earlier anaerobic phase (Wentzel et al., 1986). NADH/NAD decreases due to the presence of electron acceptor and associated ATP generation; thus ATP/ADP ratio increases. TCA cycle (concomitant glyoxylate pathway), degradation of PHB are simulated as a result of a decrease in the NADH/NAD ratio. The carbon and energy source for the cell function is from the degradation of PHB to acetate.

Polyphosphate synthesis is stimulated by the high ATP/ADP ratio and the important consequence of this increase in ATP/ADP ratio helps in the establishment of proton motive force and utilization of ATP for translocation of molecules across the

cytoplasmic cell membrane. The outline of the translocation of ions in the aerobic phase is depicted in Figure 3.

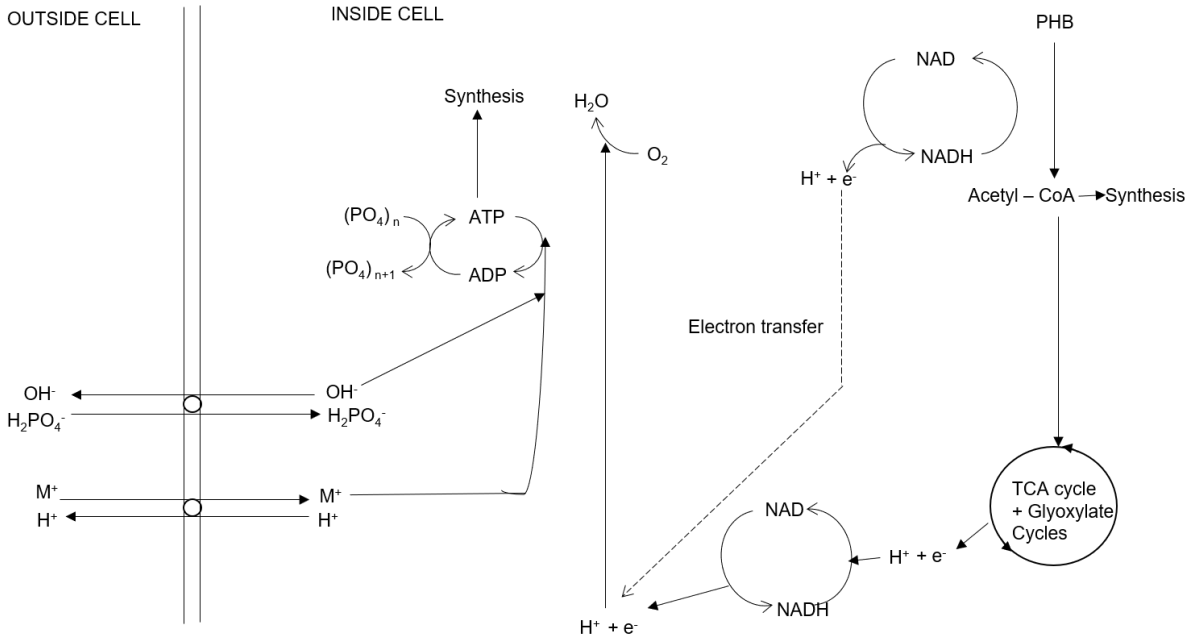

Figure 2. Ion translocation in aerobic conditions across the cytoplasmic membrane (Wentzel et al., 1986)

Based on an extensive review of the literature, the behavior of Acinetobacter species (PAOs) in the aerobic and anaerobic zone has been summarized by (Wentzel et al., 1986) as follows:

Anaerobic conditions

- Intracellular PHB synthesis
- pH remains constant without significant change
- Intracellular poly-P degradation
- One mole phosphate release is associated with an equal mole of cation release
- Phosphate release (mole) to VFA consumption (mole) tends to be 1:1
- Cation concentration (especially Mg^{2+}, K^+) increases in the bulk liquid
- VFA concentration decreases in the bulk solution
- Phosphate concentration in the bulk solution increases

Aerobic conditions

- Intracellular PHB degradation

- Bulk solution pH increases
- Intracellular poly-P synthesis
- VFA concentration increases in the bulk solution
- Phosphate concentration reduction in the bulk solution
- Cation concentration (especially Mg^{2+}, K^{+}) decreases in the bulk solution

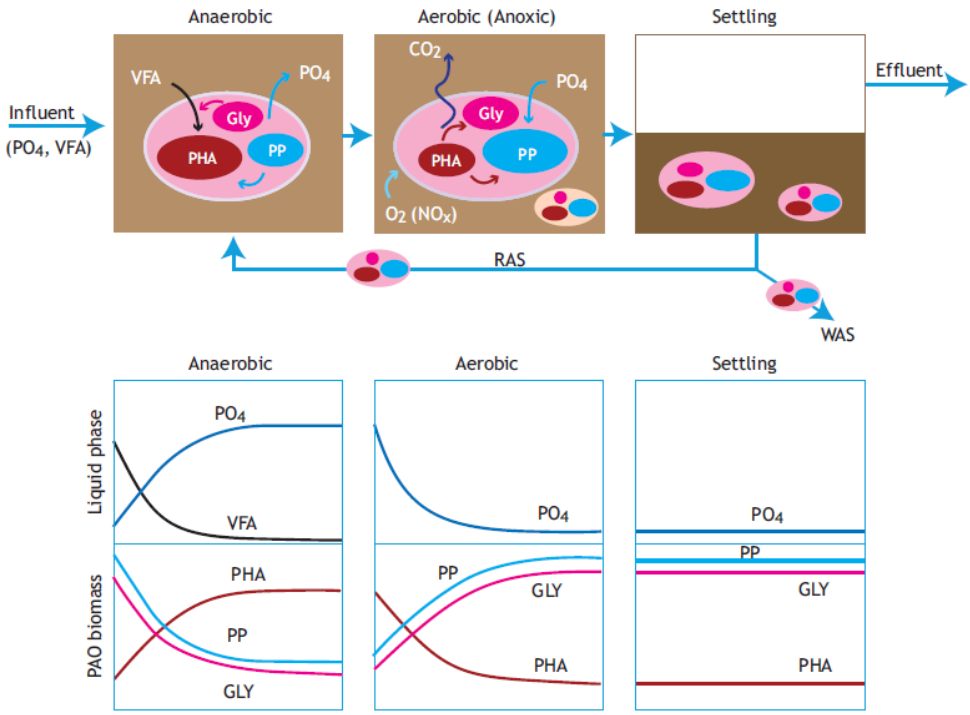

Figure 3. Schematic diagram illustrating the EBPR process in an activated sludge treatment plant (van Loosdrecht et al., 2016).

The trend of PO_4^{3-}-P (orthophosphate) and VFAs during the anaerobic, aerobic, and settling phases of the EBPR process in the liquid phase, and PAO biomass have been illustrated in Figure 3.

2.2.3 PAO, GAOs, and EBPR

PAOs outcompete ordinary heterotrophic organisms as they can store VFAs effectively in the absence of electron acceptor (Oehmen et al., 2010). The uptake of VFA by PAOs and GAOs helps in outcompeting heterotrophic organisms (Layer et al., 2019). To control the domination and abundance of ordinary heterotrophic organisms, an easily

biodegradable substrate for instance acetate must be converted to a slowly biodegradable carbon source (microbial polymers) such as Poly-Hydroxy-Alkanoates (PHA). The bacterial guilds in the deeper layers of the granules are found to store PHA and using it later for denitrification. PHB is used for cell maintenance in the absence of both external organic carbon and nitrate. PHB favors denitrification in the presence of nitrate and the absence of organic carbon. Thus PHB has found to be utilized for denitrification and cell maintenance as a carbon source in the absence of external organic carbon (Li et al., 2008).

There are different groups of competitors involved in taking up the VFAs such as PAOs (non-denitrifying and denitrifying), GAO's, and filamentous bacteria. The efficiency of Bio-P removal depends on the selection of guilds that facilitates the accumulation of phosphate under VFA uptake. The effectiveness of phosphorous removal is determined to a significant extent on the availability of VFA to the PAOs during the anaerobic phase (Jabari et al., 2016). Biological phosphorus removal can also be enhanced by the addition of metal salts in the AGS system directly in the bulk volume if required (Pronk et al., 2015).

2.3 AGS - an overview

The use of flocs for wastewater treatment is well known for more than 100 years, still, in the 1990s a qualitatively new form of aggregate was discovered and were referred to as granules (Bengtsson, et al., 2018). The properties of AGS i.e. high density and large size, makes its settling velocity to be much higher than conventional activated sludge. The high settling velocity of the granules contributes to higher biomass retention even under short hydraulic retention time (HRT) operational conditions (Zhu et al., 2018). The sub-chapter provides an overview of the wastewater treatment process with AGS.

2.3.1 Granule structure & size

In both AGS and upflow sludge blanket reactors (UASB) segregation of microbial communities occurs as a function of depth and within the different layers of the granules (Winkler et al., 2011). The changes in shear stress distribution, substrate concentration variations within granule depth favor the growth of a specific microbial guild at a

specific depth. Different microbial communities can be identified at different depths in the same reactor. SRT can be used as a selection pressure for selecting favorable microbial guilds within a reactor.

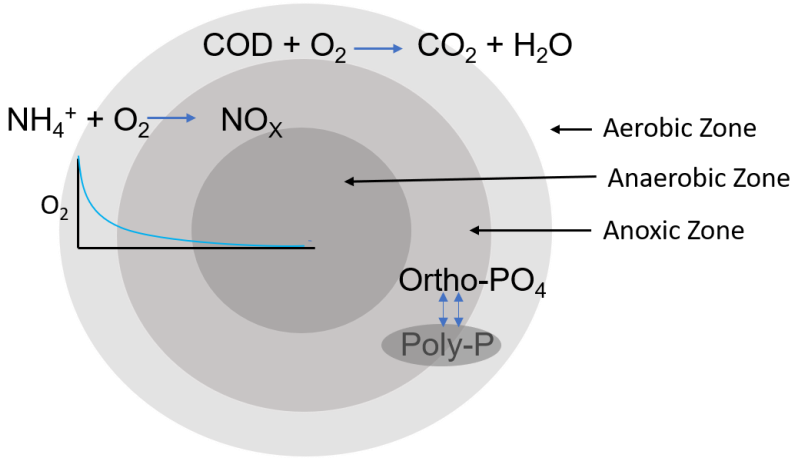

Figure 4. A typical aerobic granular structure.

Stratification of layers of different zones (aerobic, anoxic, and anaerobic) occurs as the granule size increases on account of mass transfer limitations as shown in Figure 4. Hence, the size of the granules plays an important role in nutrient removal performance. Granule size has been found to influence the microbial community in the granules (Winkler et al., 2011). The presence of the aerobic zones at the outer surface of the granules and anoxic zones in the inner layers of the granules coupled with the diffusion of the substrate for instance acetate into the deep layers of the granules enables the simultaneous nitrification and denitrification (SND) mechanism to take places in granules. The mechanism of SND in aerobic granular sludge depends on the distribution of autotrophs and heterotrophs within the granules. During the feast period, as the substrate diffuses into the granule layers, it is internally stored in the cells. These internally stored polymers are available throughout the granule during the famine period. As the autotrophs require oxygen for oxidizing ammonium, these microbes are present at the outer layers of the granules. The nitrate oxidized by these autotrophs diffuses deep into the granules, where the heterotrophs in the inner layers use the nitrate for denitrification. The complete removal of nitrogen depends on the balance between aerobic and anoxic zones within the granule layers (De Kreuk et al., 2006).

The study of three size categories of granules 0.15-0.28 mm (small), 0.28-0.45 mm (medium), granules of size more than 0.45 mm (large) observations was as follows: The medium size granules (0.24-0.45 mm) were the most preferred granular size in

terms of N, P removal (Li et al., 2018). It has been observed that the EPS secretion, diffusion of the substrate, microbial structure, and other biological characteristics of the granules are found to be influenced by the granule size. The nutrient removal efficiency varies with the size of the granules. Substrate diffusion limits in large granules hinder the denitrification process, while the small size granules favor better mobilization of orthophosphate into the inner layers of the granules.

The microporous structure of the small granules favors the diffusion of the substrate. It has been observed that the phosphorus removal in smaller granules is better than in larger granules. Smaller granules (less than 0.2 mm) has found to possess 75% of the granule volume with high phosphorous activity microbial guilds, while its only 19% for large granules (0.8mm). Hence, the smaller granules might have better phosphorus removal potential (Wu, et al., 2010). Higher TP (Total Phosphorus) content of the smaller granules indicates better phosphorous removal activity in smaller granules (Li et al., 2018). While the granule size does not tend to influence the ammonium oxidation rate, lower denitrification performance has been observed in smaller granules (<1.3 mm) (De Kreuk et al., 2006). Mass transfer limitations can be expected in granules on account of its large and compact structure (Li et al., 2008). For the same density, the nitrification and denitrification process is higher in granules of 0.7 mm than in 1.5 mm (Bin et al., 2011).

In a nitration-annamox granule, the granule size has a significant impact on the segregation of the microbial community. The anammox has been found in the fast settling and the unfavorable nitrite-oxidizing guilds in relatively smaller granules (Winkler et al., 2013). As both small and large granules are prone to the same bulk DO levels, the penetration depth of oxygen in the granules is similar. Larger granules have a smaller aerobic volume in comparison to smaller granules, as smaller granules have a higher specific surface area, therefore producing favorable conditions for annamox. The low concentration or absence of nitrite within the smaller granules helps the annamox to outcompete nitrite-oxidizing bacteria (NOB). The low aerobic volume in larger granules suppresses the NOB guilds (Winkler, et al., 2011). Theoretically, the aerobic volume available for nitrifying guilds is significantly higher in smaller granules than in the larger granules and therefore smaller granules seem to have higher nitrification capacity (Mari et al., 2014; Wilén et al., 2018).

2.3.2 Density

The presence of calcium precipitates is common in enhanced biological phosphorous removal (EBPR) systems both in AGS and activated sludge (Winkler et al., 2013). Granules at the bottom of the reactor usually have a larger diameter or high specific density which enables them to settle faster. Distinct conditions occur as a function of depth in a bioreactor. The formation of precipitates by the activity of PAOs is more prevalent in the case of AGS than in the activated sludge process. The formation of apatite precipitates in sewage treatment plants with AGS can be expected, as the pH in real WWTP is higher than in laboratory bioreactors. These precipitates within the granules increase the density of the granules thereby enhancing the overall settling characteristics.

Polyphosphate (PP), glycogen, PHB storage within the cells of PAOs has been found to influence the density of the granules (Winkler et al., 2013). Even a 1-5% increase in ash content can significantly increase the density of the granules. The denser granules thereby have comparatively higher settling velocities. The significantly higher settling velocity of the PAO dominated granules, when compared to GAO dominated granules, results in clear and distinct segregation of these granules within the bioreactor depth. Plug flow reactor with inflow feed from the bottom has been found to favor the PAO dominated granules than the GAO's, as PAO dominated granules are denser. The system fed with influent from the bottom can be optimized to selectively support the PAOs. The PAOs which settle in the bottom when compared to GAO's is enriched with organic carbon from the influent (Bengtsson et al., 2018). Plug flow reactor with inflow feed from the bottom has been found to favor the PAO dominated granules rather than the GAO's.

2.3.3 Settling Velocity

One of the selection pressures used in AGS is it’s settling velocity. Settling velocity helps in flushing out flocculent biomass and in retaining large aggregated biomass. High settling velocity acts as a selection pressure as it gives a competitive advantage to the granules rather than the flocs and it facilitates the removal of flocs (Bengtsson et al., 2018). Factors influencing the settling velocity of the granules are shape, particle size, and the difference in densities of granules and the liquid media (Winkler et al., 2013).

Settling velocity of flocculating biomass is less than 7 m/h, while it's 30 m/h for aerobic granules (Derlon et al., 2016). The settling velocity of granular sludge ranges between 10 to 100 m/h which is significantly higher than that of activated sludge (<5 m/h). The low flocculation tendency of the granules enables it to settle independently from each other even at very high biomass concentrations. Hence, the nature and behavior of granular settling are widely different from activated sludge. Granules form a compact bed directly, instead of stages as in the case of activated sludge (van Loosdrecht et al., 2016).

2.3.4 SVI

The Sludge Volume Index (SVI) is the volume occupied by 1 g of sludge after 30 min of settling (Metcalf and Eddy, 2014). Based on the settling velocity, granules can be characterized with SVI_{30} less than 90 mlg^{-1} and SVI_{30}/SVI_{10} ratio greater than 0.8 (Layer et al., 2019). The difference in SVI at 5 minutes and SVI at 30 minutes narrows eventually indicating good granulation and settling properties (Pronk et al., 2015). The high biomass concentration of AGS of about 5 times higher than activated sludge flocs has a significant influence on the SVI. The SVI after 8 minutes of settling in the case of conventional activated sludge granules is around 80-150 ml/g, while it is only 14 ml/g for granules, based on laboratory scale studies over a long-term period (De Kreuk et al., 2006). SVI of activated sludge biomass lies within the range of 80-150 ml/g, while it is 50 ml/g for AGS granules. The activated sludge flocs have a low settling velocity of 1 m/h, require high HRT to separate the biomass and the effluent in the secondary clarifier (Metcalf and Eddy, 2014).

2.3.5 External mass transfer limitations

The external mass transfer limitations are critical since DO drop as high as 22-80% occurs between bulk liquid and aggregate surface (Wilén, et al., 2004). The overall substrate consumption depends on the following process 1) transport of substrate from the bulk liquid into different layers of the granules (external mass transfer limitations) 2) mass transfer limitations within the aggregates (internal limitations) 3) consumption of substrate by the microbial community. As the substrate consumption depends on each of the above-mentioned processes in sequential order, understanding the mechanism of external mass transfer limitations is critical and essential. The availability of the substrate at the surface of the aggregates depends on the transport of

the substrate by diffusion and convection in the bulk liquid through a concentration boundary layer i.e. external mass transfer limitation. Low turbulence levels and low DO concentrations allow higher external mass transfer limitations. As granule size increases external mass transfer limitations are more observable and the authors observed higher internal mass transfer limitations in large and dense granules. Decreased biomass-specific activity or increased porosity might be the reason for the lower oxygen uptake rate in larger granules.

Substrate diffusion limits in large granules hinder the denitrification process, while the small size granules favor better mobilization of orthophosphate into the inner layers of the granules (Li et al., 2018). The diffusion of COD and nitrate is easier in smaller size granules as the mass transfer limitations are relatively low when compared to larger granules. Hence, the degradation rate is also faster in smaller granules. For instance, in large granules, if the HRT is low, it might result in incomplete denitrification**.** The poor denitrification ability of the larger granules can be attributed to the mass transfer limitations in larger granules.

2.3.6 Carbon leakage

Wagner et al., (2015) stated that "Domestic and industrial wastewater often contains diverse carbon sources along with a multitude of organic, inorganic compounds and particulate organic matter". Around 50% of the influent wastewater in the Netherlands is made of particulate slowly biodegradable COD (De Kreuk, et al., 2010). Scarce availability of diffusible organic substrate has been found to result in granules with poor settling and low nutrient removal ability. The relatively high growth of ordinary heterotrophic guilds results in low phosphorous removal and high filamentous growth (Layer et al., 2019). Hydrolysis of particulate organic carbon under anaerobic conditions is a slow process and can lead to carbon leakage, the condition in which the carbon is available at aerobic conditions (Wagner et al., 2015). Ordinary Heterotrophic Organisms (OHOs) are favored by carbon leakage, outcompeting PAO and GAO guilds, and also contribute to filamentous growth. The particulate organic carbon which is slowly biodegradable is hydrolyzed at the surface of the granules. The product of the hydrolysis which is a readily biodegradable substrate is found in the outer surface of the granules. The steep gradient in the availability of readily biodegradable substrates from outer to inner layers of the granules induces the growth of filamentous organisms.

Hence the reactor operations must consider the slow nature of the hydrolysis process in real wastewater to reduce the occurrence or likelihood of formation of filamentous guilds. Reducing the harsh selection pressure and relatively long anaerobic periods can be a solution.

2.3.7 Dissolved Oxygen

The economic considerations and the increasing stringent effluent quality standards encourage the use of low dissolved oxygen concentrations during the aerobic phase in WWTP operations (De Kreuk et al., 2006). The use of a bubble column reactor especially in large scale reactors is better than the airlift reactor due to its simplicity in design, construction and can significantly lower the capital investment required. Lowering Dissolved Oxygen (DO) levels as much as possible without causing hindrance to the nitrification process is essential to save energy when it comes to large scale wastewater treatment operations. Experiments conducted in laboratory studies have shown 40% DO saturation is desirable for both granulation and nutrient removal. Operation at 20% oxygen saturation has been observed to have the highest nitrogen removal which can be attributed to the denitrifying phosphate accumulating organisms (DPAOs). The low oxygen levels create a sufficient volume of the anoxic zone for the effective functioning of DPAO with 94% total nitrogen removal.

2.3.8 Granule Porosity

The molecular size higher than137,000 Da, 76,000 Da, and 29,000 Da have not been found to penetrate in granules of sizes 0.2-0.6 mm, 0.6-0.9 mm, 0.9-1.5 mm respectively (Zheng and Yu, 2007). The biological activity of the granules is influenced by the pore size as it dictates the diffusion limitations of the substrate into the inner layers of the granules. A positive correlation has been established between the pore size and the activity of the granules. The porosity of granules has been observed to decrease with an increase in granule size. EPS might plug the pores in large granules. The pore size distribution, availability of pores, mass transfer limitations of the substrate molecules influences the transport of nutrients and metabolites within the granules. The transportation of nutrients and metabolites is limited in larger granules when compared to small granules.

The pores and channels in the granules facilitate the transfer of oxygen into the inner layers of the granules. Tay et. al., (2002) observed that at a depth in the range of 300-500 µm, higher detection of channels and pores was possible. The presence of

obligate anaerobic Bacteroides species was used as an indicator for detecting the anaerobic layers within the granules, while AOB was observed for finding the aerobic layers. At the depth of 800-900 µm and 70-100 µm were observed to be anaerobic, aerobic layers in the granules respectively. They suggested that the plugs in channels and pores by polysaccharides might be the reason for the cell death in the inner core of the granules. The channels and pores help in interconnecting the surface and interior of the granules thereby reducing the diffusion limitations. Size optimization of the granules for efficient nutrient removal depends on balancing the aerobic and anaerobic volume in the granules. It has also been suggested that the formation of gases and fermentation products by the anaerobic bacterial community in the interior of the granules can result in granular instability and structure breakage. Granule diameter of 1600 µm has been proposed to be the optimal size of granules for efficient treatment operations.

2.4 Batch activity tests

Broad and diverse factors such as the characteristics of influent wastewater to climatic conditions can affect the removal of contaminants from the wastewater in a WWTP. Hence, there is a need to understand the influence of environmental factors on the treatment plant performance. The execution of batch activity tests performed in controlled environmental conditions can be used to understand the 1) the kinetic rates and stoichiometric parameters for the conversion of a specific compound 2) to study the possible interactions, for instance, symbiosis and competition between different microbial populations. The complexity of the batch activity tests performed depends on the physiology and the interaction of the microbial population involved. For instance, to study the metabolic activity of PAOs demands biochemical environments as diverse as aerobic, anoxic, and anaerobic.

Phosphorus removal potential of activated sludge can be characterized by conducting phosphorus release under laboratory batch activity tests (Tykesson & Jes, 2005). The potential of bio-P function in the treatment plant can be assessed by the capacity of the sludge to release phosphorus under controlled environmental conditions in the lab. Optimization of plant operation is possible if the activity tests are performed regularly. The influence of toxic components on the removal performance can be assessed and the results from the tests can be used for creating a simple modeling tool for the treatment plant considered.

3 Materials and Methods

Batch activity tests under controlled environmental conditions were carried out to assess the maximum capacity of the microbial guilds in performing bio-phosphorous removal, nitrification, and denitrification. The experiments were performed in lab-scale test batch reactors (1000 ml storage bottles). The chapter discusses the process of how the experimental protocol was developed to perform the batch activity test, its limitations, and subsequently the final method which was employed to perform the tests. The experiment protocol follows the method by van Loosdrecht et al., (2016) with some modifications to answer the specific research questions/objectives.

3.1 Synthetic wastewater composition

The composition of synthetic wastewater prepared has been listed in Table 1. 1 ml of micronutrient solution which was a mixture of chemicals mentioned in Table 2 was added to 1L of synthetic wastewater prepared (García, 2019). The Mg:K:P ratio of nutrients in synthetic wastewater has been maintained at 1:3:3 (in terms of moles), to provide sufficient macronutrients for microbial uptake.

Table 1. Synthetic wastewater composition

Nutrient	**Concentration (mg/l)**
KH_2PO_4	109.85
KNO_3-N (for anoxic)	20
$NaNO_2$-N (for anoxic)	20
$CaCl_2$	14
$MgSO_4.7H_2O$	90
$FeSO_4.7H_2O$	20

Table 2. Micronutrient solution constituents

Nutrient	**Concentration (g/l)**
H_3BO_3	0.05
$ZnCl_2$	0.03

$Cucl_2$	0.05
$MnSO_4.H_2O$	0.05
$(NH_4)_6Mo_7O_{24}.4H_2O$	0.05
$Alcl_3$	0.05
$Nicl_2$	0.05
$Cocl_2.6H_2O$	0.05

3.2 Experiment procedure

3.2.1 Reactor setup

The reactor used for the experiments was 1000 ml glass bottles (PYREX™ Reusable Media Storage Bottles), with 900 ml working volume. The reactors were placed in a water bath maintained at 20^o C using a temperature controller (Lauda E100). A diffuser stone was used for sparging N_2 gas and air, for anaerobic and aerobic phases, respectively. The pH was maintained in the range 7±0.1 using a VWR pH 110 meter, while DO was monitored with MultiLine® Multi 3510 IDS meter. Centrifugation (Sigma 4-16KHS) was used for the separation of sample biomass from the aqueous phase. The sample was placed in the centrifuge at 4500 rpm for 1 minute. The aqueous phase after centrifuging was filtered with a 0.2 µm filter using a 5ml syringe. The experiment setup was as illustrated in Figure 5.

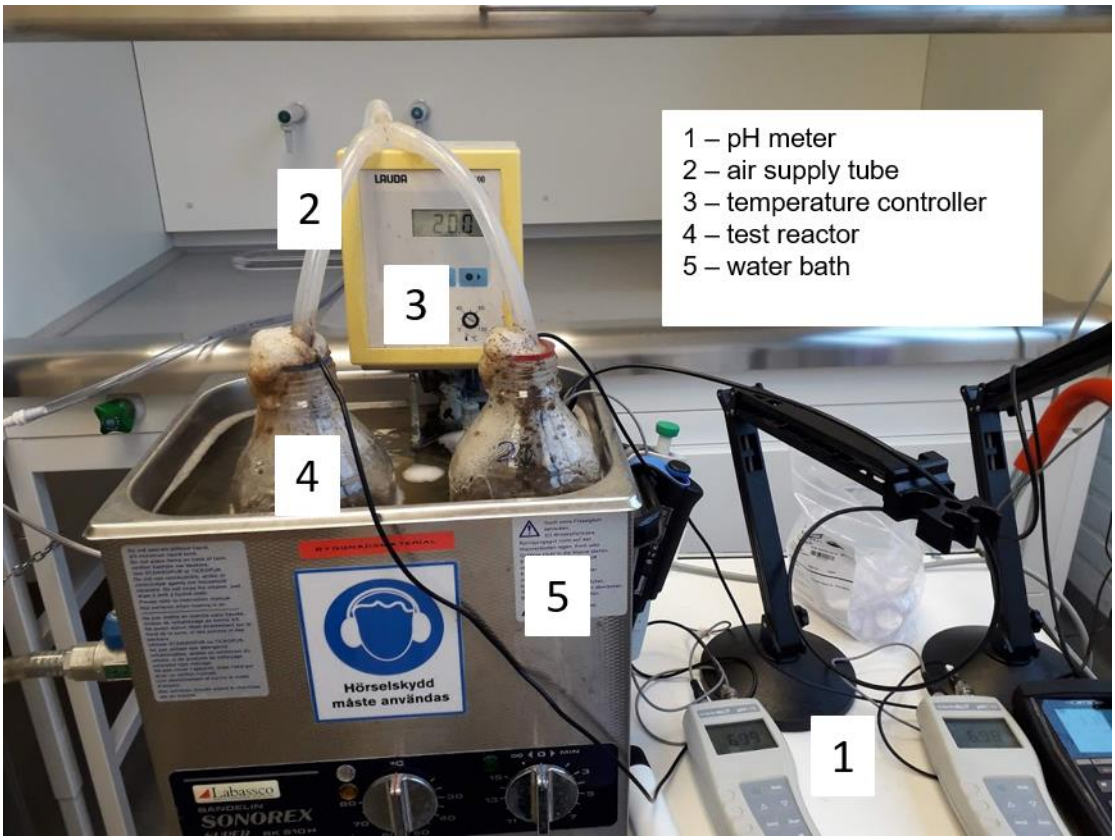

Figure 5. Experimental setup.

3.2.2 Bio-P activity test

The activity test was performed in the following steps:

Step 1: The sludge stored in the refrigerator was washed as described in section 3.3.2 of the report.

Step 2: The sludge was transferred to the reactor setup as outlined above in section 3.2.1 of the report.

Step 3: The experiment started with a pre-aeration phase which involved aerating the granules at saturated DO levels for 1 hour. The pH was monitored and controlled. Orthophosphate was added at the time (t = -60 minutes) as mentioned in section 3.2.5.

Step 4: The anaerobic phase was started by turning off the aeration and sparging N_2 gas with the diffuser stone as mentioned earlier in section 3.2.1. Sodium acetate was added as a carbon source.

Step 5: Samples were taken at pre-determined intervals (at times, t = 0, 10, 20, 30, 45, 60, 75, 90, 120 minutes).

Step 7: The samples were analysed for the ions NO_3^--N, NO_2^--N, PO_4^{3-}-P, K^+, Mg^{2+}, and acetate using Dionex ICS 900. The sample preparation steps involved were described in section 3.3.

Step 8: After the completion of the Bio-P anaerobic release activity test, the same sludge was used for aerobic uptake tests. The supply of N_2 gas was turned off and aeration was turned on.

3.2.3 Nitrification test & denitrification activity test

Ammonium was added at the start of the test. The conversion of ammonium to nitrite and nitrate was analyzed with IC as mentioned in step 7 of section 3.2.2. While during the denitrification activity test NO_3^--N and acetate were added at the start of the test. The conversion of nitrate (electron acceptor) into nitrogen gas with the consumption of acetate (electron donor) was analyzed with IC as described in step 7 of section 3.2.2.

3.3 Sludge washing

3.3.1 Initial method

The concentration of activated sludge present in a bioreactor was given in terms of mixed liquor suspended solids (MLSS) and mixed liquor volatile suspended solids (MLVSS) concentrations (Metcalf and Eddy, 2014). The Mixed Liquid Suspended Solids (MLSS) concentration taken from the WWTP might be different from the target MLSS concentration at which the experiment was planned to be performed. For instance, if the assumed MLSS concentration of the sludge taken from the wastewater treatment plant was X g/l (say 8 g/l) and if the desired target concentration of MLSS for the lab experiment was 0.25 X g/l (2 g/l). The procedure followed for sludge preparation has been illustrated in Figure 2. The steps to be performed to arrive at the target sludge concentration for the experiment were as follows:

Step 1: After harvesting, the sludge was stored in the refrigerator and was taken out before the experiment.
Step 2: The sludge was filled in a measuring cylinder as shown in Figure 6a.
Step 3: The sludge was allowed to settle for 30 minutes. This step enabled the effective separation of biomass and wastewater as shown in Figure 6b.
Step 4: The supernatant water was decanted as shown in Figure 6c and refilled again with synthetic wastewater as shown in Figure 5d.
Step 5: Steps 2, 3, and 4 were repeated twice with prepared synthetic wastewater.

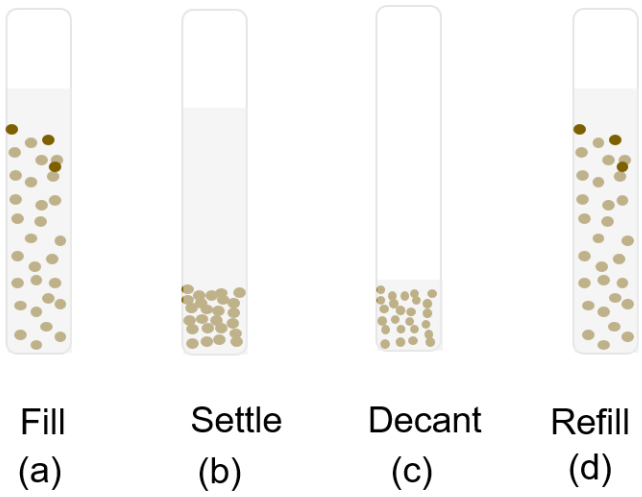

Figure 6. Sludge washing steps.

Step 6: The sludge (synthetic wastewater + biomass) was transferred to a larger container using a funnel.

Step 7: The contents were mixed by shaking the container more than 3 times.

Step 8: Again, the contents were transferred from the large container to batch reactors using the funnel as shown in Figure 7.

Step 9: The sludge was diluted by increasing the volume of synthetic wastewater to the target MLSS concentration.

The method involved several steps where the sludge was transferred from one vessel to another. To have representative results it was very important to get a homogenous sample of granules. The 5L bucket, for instance, had a small opening so when sludge was transferred from that, it might have left larger granules in the bucket since they settled very fast. Hence it was not a representative sample of the biomass. So instead, the entire volume of sludge was transferred to a larger beaker that can be mixed with a large spoon to get a homogenous mix of granules. After which it was transferred to a measuring cylinder for further steps.

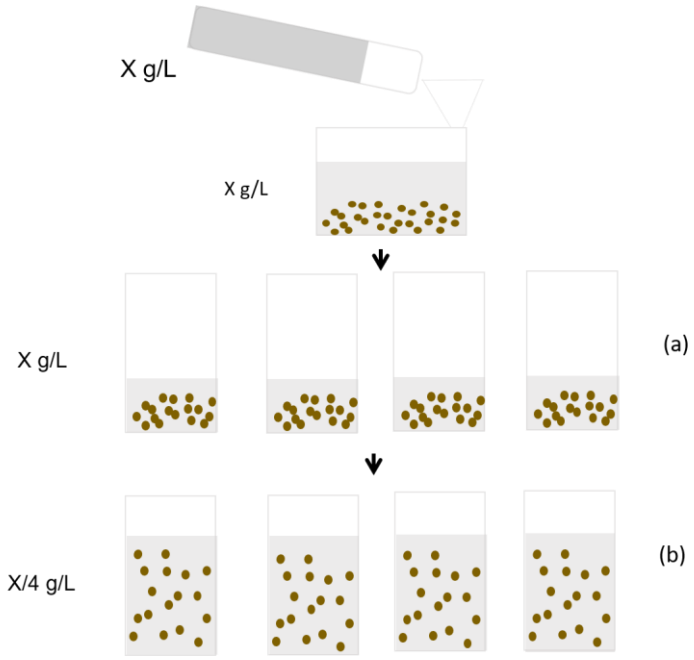

Figure 7. Steps in sludge preparation. a) the sludge after transfer from the container. b) the sludge from step a) is diluted again with synthetic wastewater to achieve the desired concentration.

3.3.2 Sludge washing-Final method

3.3.2.1 Washing Mixed Sludge

Step 1: The bucket of stored sludge (5L volume) was taken out of the refrigerator.

Step 2: The contents were transferred into a large bucket with a very big opening.

Step 3: The sludge was stirred thoroughly.

Step 4: The desired quantity of sludge was transferred to a 1000 ml measuring cylinder.

Step 5: Synthetic wastewater was added to the sludge.

Step 6: The sludge was allowed to settle for 30 minutes, to facilitate the separation of biomass and the water.

Step 7: The supernatant was separated from the biomass.

Step 8: Again, synthetic wastewater was added to the biomass, and step 6 and 7 was repeated.

Step 9: The washed sludge was transferred to the experiment beaker using a funnel.

Step 10: The volume was adjusted to 900 ml by adding more synthetic wastewater.

3.3.2.2 Washing sieved granules

Step 1: The bucket (5 L volume) with granules was taken out from the refrigerator.

Step 2: The granules were segregated into different size fractions by allowing the sludge to pass the sieve. The diameter of the sieve used was 2 mm for this work.
Step 3: Tap water was used to wash the sludge for about 5 times so that the granules were well sieved.
Step 4: The granules retaining on the sieves were transferred to an aluminium crucible using a spoon.
Step 5: From the crucible, the granules were again transferred to the experiment bottles using a funnel. Synthetic wastewater was added in the funnel for quick transfer of granules into the test bottles.
Step 6: The working volume was adjusted to 900 ml by adding more synthetic wastewater.

3.4 pH Control

pH was not controlled in initial experiments. The possibility of pH affecting the biological phosphorus uptake and release is significant and hence, to eliminate this uncertainty, pH was controlled in later experiments. Controlling pH also helps in providing similar environmental conditions across various tests performed. The steps involved in controlling pH were as follows:
Step 1:The pH was checked using a pH electrode after adding KH_2PO_4 during the pre-aeration phase of the experiment.
Step 2: In case of pH being lower than neutral pH, say 5.6, 100-200 µL of a strong base (1 M solution) was added.
Step 3: The pH was maintained within the target range of 6.9-7.1 by adding 30 µL acid or base to decrease or increase the pH accordingly.
Step 4: During the anaerobic phase, after the addition of sodium acetate, the pH values drop below the target range, and hence step 3 was repeated to maintain the pH within the target range.

3.5 Sample preparation for IC

The steps involved in sample preparation for IC were as shown in Figure 8.
Step 1: 5-7 ml of sample were taken out from the experiment reactor at pre-determined intervals using a 50ml syringe.
Step 2: The sample from step 1 was stored in a labeled test tube.

Step 3: The sample was placed in the centrifuge at 4500 rpm (rotations per minute) for about 1 minute. This step allows the effective separation of biomass and water.
Step 4: The supernatant thus separated was transferred into a 5ml syringe.
Step 5: The separated supernatant was filtered through a 0.2 µm filter and the collected sample was kept in the test tube.

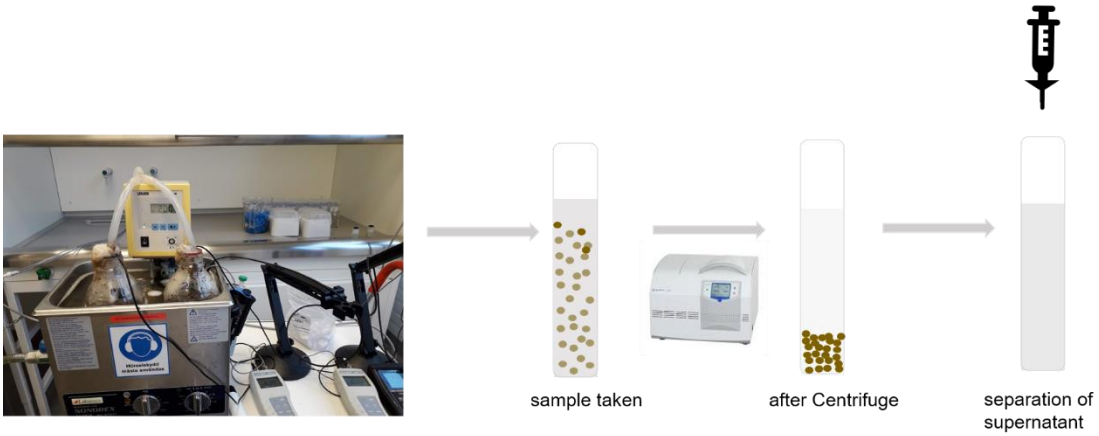

Figure 8. Sampling method.

Step 6:1ml of the filtered sample was transferred to IC (well rinsed) vials using 1 ml micropipette.
Step 7: The sample was diluted by adding 6ml of MilliQ using a micropipette.
Step 8: Vials were closed with the caps with the help of a special small rod, to make sure there were no air bubbles left.
Step 19: The vials were placed in the autosampler of the IC set-up.

3.6 Analyzing the samples in IC

Step 1: The anion pumps, cation pumps, and autosampler were powered on.
Step 2: The chromeleon software was opened on the computer.
Step 3: ‘Instruments’ option was selected
Step 4: The option was turned on from ‘disconnected’ to ‘connected’ for anion pump, cation pump, and autosampler.
Step 5: The pumps were turned ‘on’ in the software for anion and cation pump.
Step 6: The monitor baseline option for both anions and cations were selected.
Step 7: 15-20 minutes of the waiting period was followed for the baseline to stabilize.
Step 8: The cursor was navigated to ‘Data’ and a new sequence was created.

Step 9: The details of each sample were entered, and it was ensured that the dilution factor is set to 1.

Step 10: It was ensured that the 'Stop' option was selected for the last position of the vial.

Step 11: The position of the vials were filled using the 'Fill down' option and it was ensured that the numbers were in ascending order from 1 to n samples.

Step 12: It was checked that the baseline conductivity stabilized to zero after 15-20 minutes of monitoring. The baseline value was ensured to be below 2 µS. The 'Monitor baseline' option was deselected.

Step 13: The sequence created was saved in the software and the details were entered in the logbook.

Step 14: 3 standard samples of known concentration were placed with the unknown samples in the autosampler for calibration.

Step 14: The 'Start' option was selected to start the analysis of the sequence created.

3.7 Adding external carbon and phosphate source

Step 1: Stock solution of sodium acetate and KH_2PO_4 were prepared. It was ensured that the quantity of chemical salt added was below the maximum saturation limits to avoid precipitations in the stock solutions.

Step 2: The required volume of the prepared stock solution to be added for the specific experiment was calculated.

Step 3: The exact volume of the solution was added using micropipette at pre-determined intervals (acetate during the anaerobic phase; phosphate during the aerobic phase) and samples were taken immediately.

In the initial method, the samples were taken out during the experiment as soon as the stock solution had been added to the batch reactor. Enough time was probably not provided for the effective mixing of ions as the measured concentration of ions and expected concentration based on calculations were different. Hence, The ion concentration was underestimated. Instead, samples were taken 2 minutes after the addition of the stock solution.

3.8 MLSS and MLVSS test

Step 1: A new glass filter paper was weighed, and 4 decimal places were recorded on the balance.

Step 2: 150 ml of sludge from the test reactor was taken using a 50 ml syringe and was stored in the test tubes. It was ensured that the tube connected to the syringe (to take out sludge with) was higher than 1 cm so that even relatively larger granules were not left out.

Step 3: The test tube was shaken well, and the contents were transferred to a larger plastic beaker.

Step 4: Electric mixer was used to evenly mix the granules into a homogeneous slurry.

Step 5: The weighted filter was placed in the filtering equipment.

Step 6: 3 ml of mixed sludge from step 3 was taken for filtration. It was ensured that the tip of the pipette was cut (using scissors) so that a larger fraction of granules, if any, could enter via the tip of the pipette.

Step 7: The sludge was filtered using the filtering equipment. MilliQ water was used to flush out the sticking sludge from the filtering equipment. It was ensured that no biomass was stuck on the sides of the filtering equipment.

Step 8: The filter paper was placed in an aluminium crucible after filtering the sample. Step 1-8 were repeated in triplicates.

Step 9: The aluminium crucible was placed in the oven at 105^{o}C for over a minimum of 4 hours or it was left in the oven overnight.

Step 10: The crucible form the previous step was cooled in a desiccator and the filter paper was weighed.

Step 11: The crucible was placed in a 550^{o}C oven for at least 1 hour.

Step 12: The samples were cooled in the desiccator and the filter papers were weighed.

Step 13: The formula mentioned in Appendix-D of the report was used to calculate the MLSS and MLVSS for each sample. Microsoft Excel was used for quick calculation and for presenting the average value from triplicates.

Limitations of the procedure were as follows:

1. When new glass filter papers were used sometimes there was a loss in weight of the filter when it was placed in the oven and furnace, introducing an error source in the measured weight. To adjust for this error a correction factor was

developed, and the detailed calculations can be referred by the reader in Appendix-D.

2. When the MLSS concentration was very high (> 20 g/L), it was very hard to filter the sludge sample and took a lot of time. To solve this issue, the sludge was diluted 10 times (1ml of sludge sample + 9 ml MilliQ) so that the sludge could be easily transferred through the filter. The dilution factor of 10 has been introduced in the calculations to include the effect of this step. The detailed calculation has been explained in Appendix-D.

The correction factors suggested were added to the calculations in the final method.

3.9 Kinetic and stoichiometric parameters estimation

The kinetic and stoichiometric parameters can provide information not only about the biomass activity in different environmental and operational conditions but also hints about the dominant microbial community present in the sludge sample. Based on past batch activity test studies in the literature, with acetate at 20°C and pH 7, the P-release/C up-take in P-mol C-mol^{-1} was found to suggest the dominant metabolism in the sludge sample as listed in Table 1. Theoretical acetate consumed i.e. 3.4 mg of COD for every 1 mg of nitrate utilized from simultaneous denitrification. Higher P-release/C up-take ratio (>0.5 P-mol C-mol^{-1}) might indicate a dominant PAO activity. While a lower P-release/C up-take ratio might be due to one of the following reasons 1) abundant presence of GAO's 2) electron acceptor intrusion, for instance, oxygen, nitrate, nitrite 3) addition of chemical salts for phosphorous removal and sometimes 4) with the presence of inhibitory or toxic compounds The anaerobic stoichiometric parameter P-release/C up-take ratio ($Y_{AcPO4,\ An}$) has been calculated using the PO_4^{3-}-P released and acetate consumed during the anaerobic period as shown in equation 4 (van Loosdrecht et al., 2016). The estimation of kinetic and stoichiometric parameters has been made using Microsoft Excel.

$$Y_{AcPO4,\ An} = \frac{P_{released}}{S_{Ac,cons}}$$

$$= \frac{(PO4_{final} - PO4_{ini})}{(S_{Ac,ini} - S_{Ac,final})} \ldots\ldots\ldots \text{equation [4]}$$

Where,

$Y_{AcPO4,\ An}$ is the $P_{released}$ to acetate uptake ratio

$P_{released}$ is the PO_4^{3-}-P released for acetate uptake and anaerobic cell maintenance requirement, mg PO_4^{3-}-P $L^{-1}h^{-1}$

$PO_{4,ini}$ is the concentration of the PO_4^{3-}-P in the bulk liquid at the beginning of the test, mg L^{-1} h^{-1}

$PO_{4,final}$ is the concentration of the PO_4^{3-}-P in the bulk liquid at the end of the test, mg L^{-1} h^{-1}

$S_{Ac,cons}$ is the concentration of the acetate consumed during the test, mg L^{-1} h^{-1}

$S_{Ac,ini}$ is the concentration of the acetate present in the bulk liquid at the beginning of the test, mg L^{-1} h^{-1}

$S_{Ac,final}$ is the concentration of the acetate present in the bulk liquid at the end of the test, mg L^{-1} h^{-1}

Table 1. P-release/C up-take ratios and the corresponding metabolism

P-release/C up-take (P-mol C-mol^{-1})	Dominant metabolism
<0.25	GAO dominated metabolism
0.25-0.50	Intermediate PAO-GAO metabolism
>0.50	PAO dominated metabolism

For the Phosphorous release/acetate uptake (P-release/C up-take) ratio calculation, total PO_4^{3-}-P release rate i.e. PO_4^{3-}-P release due to acetate uptake + secondary PO_4^{3-}-P release for anaerobic maintenance requirement has been considered instead of net PO_4^{3-}-P release rate which is PO_4^{3-}-P release due to acetate uptake alone. Net PO_4^{3-}-P release rate could not be ascertained, as for most of the tests secondary PO_4^{3-}-P release rate could not be calculated as acetate was not depleted completely during the test duration. Hence, the P-release/C up-take ratio calculated for the tests was an overestimate.

3.10 Experiment set-up

The environmental conditions can affect and influence the batch activity tests as mentioned in chapter 2 of the report. As several parameters can influence the batch activity tests, to ascertain the optimal environmental conditions, a set of parameters were controlled for instance temperature, dissolved oxygen as shown in Figure 9, while

some parameters were varied during the test to find its influence on the batch activity tests performed.

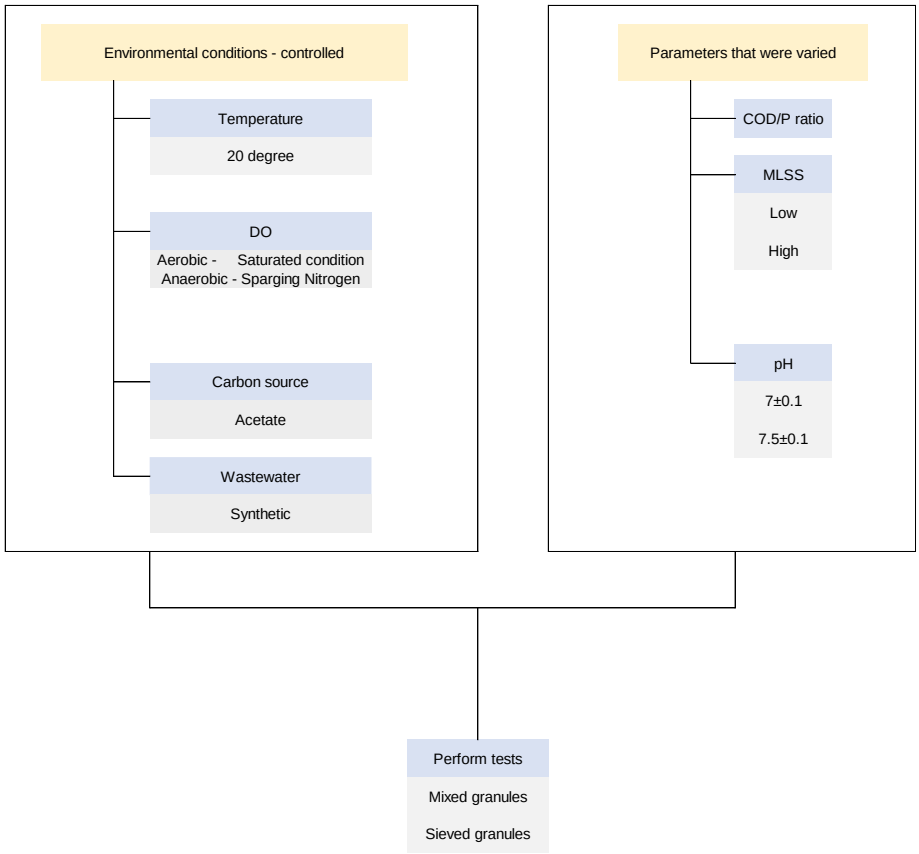

Figure 9. The parameters (environmental conditions) that were controlled and monitored during the test: temperature, carbon source, and the parameters that were varied during the test are listed. Tests were performed with mixed and sieved granules at controlled environmental conditions and by changing the variable parameters to study its influence on granules performance.

3.10.1 Effect of influent COD/P on anaerobic PO_4^{3-}-P release kinetics

The objective of this set of experiments performed was to study the effect of influent carbon/phosphorous (COD/P ratio) on the anaerobic PO_4^{3-}-P release rate in mixed granules. All the experiments were performed on the same day (03-10-2020). The carbon source for the experiment was acetate while the phosphorous source was in the form of orthophosphate (PO_4^{3-}-P). To test the effect of influent COD/P ratio, the plan was to add the same amount of PO_4^{3-}-P (40 mg/L) for all the 4 tests, while COD (in terms of acetate) was varied with 100, 200, 300, 150 mg/L for tests 1, 2, 3, and 4, respectively. It has been theoretically calculated according to stoichiometry that the

oxygen required (COD) to oxidize 1 g of acetate is 1.07 O_2 and acetate will be given in terms of COD throughout the report. pH was not controlled during the experiments. DO was monitored as mentioned in section 3.2.1 of the report. The pre-aeration phase was approximately 30 minutes and 40 mg/L of PO_4^{3-}-P was added 20 minutes before the start of the 60 minutes anaerobic phase. Samples were taken instantaneously after adding acetate and PO_4^{3-}-P solution to the test reactors.

3.10.2 Effect of MLSS on anaerobic PO_4^{3-}-P release kinetics

3.10.2.1 Mixed sludge

The objective of the set of experiments performed was to observe the effect of MLSS on anaerobic PO_4^{3-}-P release activity in mixed granules. Eight tests were performed with different MLSS concentrations in two different days (First 4 tests on 27-11-2020 and the second 4 tests on 11-12-2020). The influent COD/P ratio at the start of the test was planned to be maintained the same for all the experiments (COD: 50 mg/L PO_4^{3-}-P: 25 mg/L). The experiment started with the pre-aeration phase of 1 hour, followed by 2 hours of anaerobic phase. PO_4^{3-}-P (25 mg/L) was added at the start of the pre-aeration phase, while COD (50 mg/L) was added at the start of the anaerobic phase.

3.10.2.2 Sieved granules

The objective of the set of experiments performed was to observe the effect of MLSS concentrations on anaerobic PO_4^{3-}-P release in sieved granules. Eight tests were performed with different MLSS concentrations in two different days (First 4 tests on 17-12-2020 and the second 4 tests on 20-01-2020).

3.10.3 Batch activity test with mixed granules

3.10.3.1 Bio-P activity test

The objective of the set of experiments performed was to study the bio-P activity in mixed sludge, both anaerobic PO_4^{3-}-P release and aerobic PO_4^{3-}-P uptake activity. The activity test was performed in two test reactors with mixed sludge on the same day (25-02-2020). pH was controlled manually at 7.5±0.1 as mentioned in section 3.4. The test started with a 1-hour pre-aeration phase, followed by 3 hours of anaerobic phase and 2 hours of aeration phase. The PO_4^{3-}-P of 25 mg/L was added at the start of the pre-aeration phase, while 200 mg/L COD was added at the start of the anaerobic phase as mentioned in section 3.2.

3.10.3.2 Nitrification and denitrification activity test

The objective of the set of experiments performed was to study the nitrification and denitrification batch activity tests in mixed granules and it was performed on 25-02-2020. pH during the study was maintained above 7.5. The experiment started with a pre-aeration phase of 1 hour followed by aeration phase of 90 minutes and an anaerobic phase of 90 minutes. 40 mg/L of NH_4^+-N, 5 mM of $NaHCO_3$, 10 mg/L of PO_4^{3-}-P was added at the start of the aerobic phase and 200 mg/L of COD at the start of the anaerobic period.

3.10.4 Effect of pH

The objective of the set of experiments which was performed on 05-02-2020 was to study the effect of pH on anaerobic PO_4^{3-}-P release. Batch activity tests were performed at two different pH 7.5±0.1 and 7±0.1 to test the effect of pH on granule activity. Total Solids (TS) and Total Volatile Solids (TVS) were used as a measurement of granules concentration in test reactors instead of MLSS and MLVSS. The method of measurement has been explained in Appendix-E of the report. The measurement of TS was considered due to the non-availability of filter paper on the week of the experiment. The PO_4^{3-}-P of 25 mg/L was added at the start of the pre-aeration phase, while COD of 200 mg/L was added at the start of the anaerobic phase as mentioned in section 3.2.

3.10.5 Effect of Granule size

3.10.6 Bio-P activity in sieved granules

Bio-P batch activity tests to compare the PO_4^{3-}-P release, PO_4^{3-}-P uptake of different granule sizes in synthetic wastewater was performed on 31-01-2020, and 11-03-2020 and with real wastewater on 11-01-2020.

The pH was maintained at 7 ± 0.1 throughout the experiment phases for the tests conducted on 31-01-2020 and at 7.5± 0.1 for tests performed at 11-01-2020 and 11-03-2020. The PO_4^{3-}-P of 25 mg/L was added at the start of the pre-aeration phase for all the 6 tests performed. The COD of 100 mg/L was added as a carbon source at the start of the anaerobic phase for tests performed on 31-01-2020 while it was 200 mg/L, for tests performed on 11-01-2020 and 11-03-2020. The data corresponding to the aerobic phase (PO_4^{3-}-P uptake) was not analysed due to the COVID-19, which caused limited access to the laboratory. Two granule sizes small (< 2 mm) and large (> 2 mm) were

considered. Analysis of the results has been made between different granule sizes performed on the same date.

3.10.7 Nitrification & denitrification in sieved granules

Batch activity tests to assess the nitrification activity in different granule sizes (large and small) were performed. 40 mg/L of NH_4^+-N was planned to be added at the start of the test but instead, 100 mg/L of NH_4^+-N was added due to miscalculations. Sodium bicarbonate was not added to maintain alkalinity, but pH was controlled manually near 7±0.1. The experiment duration was for 90 minutes. To test the maximum denitrification rate in different granule sizes (small and large granules as mentioned earlier), experiment with granules > 2 mm and granules < 2 mm were performed in two separate reactors.

3.11 Uncertainties and error sources

The experimental work involves several steps from sampling to chemical analysis. All steps will introduce uncertainty which affects the results. An attempt has been made to acknowledge these sources of error and relevant correction factor (i.e. the factor that is multiplied with a result to correct a known systematic error) and standard deviations from the mean value has been introduced wherever possible. For instance, correction factors are included for IC results, while error bars are introduced in graphs to include the measurement errors from pipetting. For the detailed explanation of the calculations performed, the reader can refer to Appendix-B and Appendix-C of the report. The standard deviation as a result of uncertainty from pipetting is about ± 6% of the result values stated in the report and these standard deviations have been used in the graphs as error bars.

4 Results and discussions

The results from the method development process and the developed method are presented. Analysis and discussions of the critical kinetic and stoichiometric parameters have been made to understand the granule performance better.

4.1 Effect of influent COD/P on anaerobic PO_4^{3-}-P release kinetics

The influent COD/P ratio at the start of the anaerobic period calculated theoretically (based on the chemical salts added) and the measured ion concentration (using IC was as shown) in Table 2. One reason that could have caused the difference in the expected and observed influent COD/P ratio was that during the test, samples were taken instantaneously after adding the acetate and PO_4^{3-}-P solutions, therefore enough time was not provided for complete assimilation of ions throughout the test reactors. The other reason could be that PO_4^{3-}-P added at the start of the pre-aeration phase, while COD was added during the start of the anaerobic phase. The PO_4^{3-}-P taken up during the pre-aeration phase was not accounted for, during the expected COD/P calculation as it was different for each test, resulting in a different COD/P ratio than the theoretical ratio calculated.

Table 2. Theoretically calculated and measured COD/P ratio, kinetic and stoichiometric parameters of the tests with different COD/P ratio.

Test	MLSS (g/L)	COD/P (theoretical)	COD/P (measured)	COD up-take (mg COD g $MLSS^{-1}$ h^{-1})	PO_4^{3-}-P release (mg PO_4^{3-}-P g $MLSS^{-1}$ h^{-1})	Measured P-release/C up-take (P-mol C-mol^{-1})
1	5	2.5	3	10	5.9	0.57
2	2	5	10	48	3.4	0.07
3	2	7.5	30	15	3.1	0.20
4	5	3.75	9	14	4.0	0.38

The pH during the anaerobic phase was varying between 7-7.5 as it was not controlled during the experiment, due to the Bio-P activity. The P-release/C up-take (PO_4^{3-}-P

released/acetate consumed) for tests 1, 2, 3, and 4 were 0.57, 0.07, 0.20, and 0.38 P-mol C-mol^{-1}, suggesting PAO dominant metabolism in the test reactor 1 and GAO dominant metabolism in test reactors 2, 3 and 4 respectively as shown in Table 2. PO_4^{3-}-P uptake could not be measured accurately as the samples were taken instantaneously after adding the PO_4^{3-}-P solution to the test reactors. The correlation between PO_4^{3-}-P release and K release was 0.9, -0.4, -0.01, and 0.65 for tests 1, 2, 3, and 4 respectively. The difference in PO_4^{3-}-P release rate in tests 1, 2, 3, and 4 could not be singled out as the effect of the COD/P ratio alone since pH was not controlled during the tests. The change in pH affects the Bio-P activity, hence if the fluctuations in pH are ignored, it can be seen that the PO_4^{3-}-P release rate and P-release/C up-take ratio are higher in test reactor 1, which had a lower influent COD/P ratio. The trend of PO_4^{3-}-P release and COD consumption in the test reactors 1, 2, 3, and 4 have been shown in Figure 10 a, b, c, and d respectively.

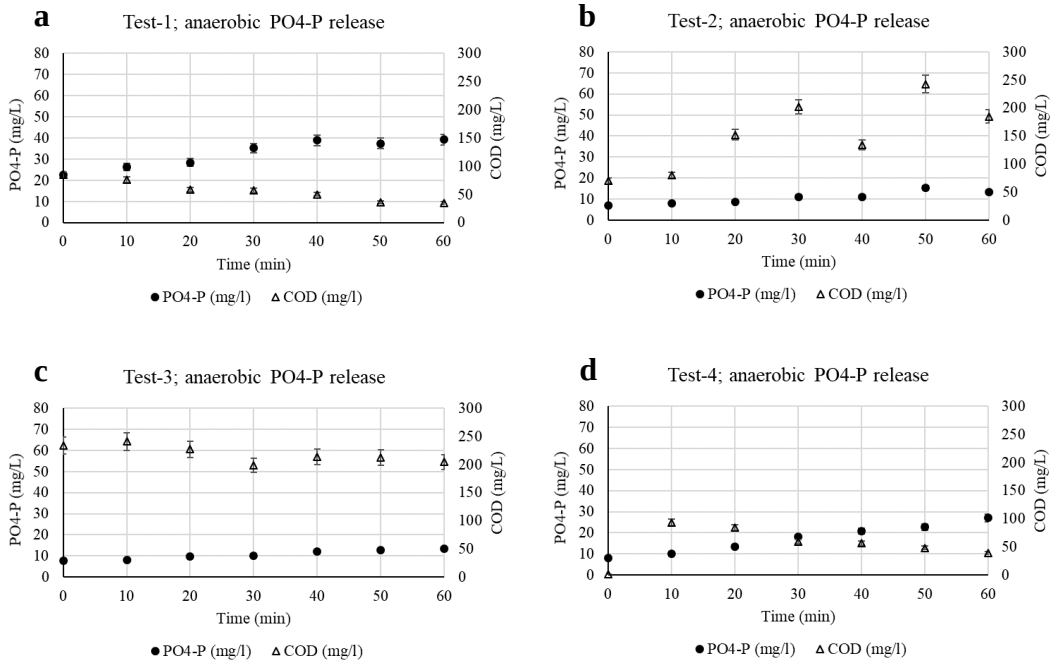

Figure 10. a, b, c and d show the trend of anaerobic PO_4^{3-}-P release and COD uptake during the anaerobic period at measured influent COD/P ratio 3, 10, 30 and 9 respectively.

4.2 Effect of MLSS on anaerobic PO_4^{3-}-P release kinetics

4.2.1 The effect in mixed granules

The MLSS concentrations of the sludge for test reactors 5-12 respectively as shown in Table 3. The trend in the PO_4^{3-}-P release and COD utilization during the anaerobic period were as shown in Figure 11. a-h for the tests 5-12 respectively. The maximum PO_4^{3-}-P release rate of 3.3 and 4.3 mg PO_4^{3-}-P g $MLSS^{-1}$ h^{-1} was observed in the test reactor 10 and 12 respectively. Both the test reactors were with relatively very low MLSS (0.3 g/L in both the test reactors). The P-release/C up-takeratio for test reactors 10 and 12 were 0.05 and 0.59 P-mol C-mol^{-1} suggesting GAO dominated metabolism in test reactor 10 and PAO dominated metabolism in test reactor 12 respectively. In tests 6, 9, and 11 there was no PO_4^{3-}-P release (even negative values), and in all the three reactors the MLSS concentration was low at 0.8, 0.3, and 0.3 g/L respectively.

Table 3. MLSS, Kinetic and stoichiometric parameters of the tests 5-12.

Test	MLSS (g/L)	COD up-take (mg COD g $MLSS^{-1}$ h^{-1})	P release (mg PO_4^{3-}-P g $MLSS^{-1}$ h^{-1})	Measured P-release/C up-take (P-mol C-mol^{-1})
5	2.8	2.8	1.4	0.50
6	0.8	24.4	-0.6	-0.03
7	13.0	7.4	1.8	0.31
8	11.4	9.7	3.3	0.36
9	0.3	26.4	-1.6	-0.06
10	0.3	63.8	3.3	0.05
11	0.3	37.3	0.0	0.00
12	0.3	7.3	4.3	0.59

The maximum P-release/C up-take ratio of 0.50, and 0.59 indicating PAO dominated metabolism were observed in the test reactors 5, and 12 respectively out of which one test reactor was with high MLSS (test 5) and one with low MLSS (test 12). The PO_4^{3-}-P release rate in the test reactors 7 and 8 (with high MLSS of 13.0, 11.4 g/L) were 1.8 and 3.3 mg PO_4^{3-}-P g $MLSS^{-1}$ h^{-1}. The P-release/C up-take ratio was 0.3 and 0.36 P-mol C-mol^{-1} suggesting intermediate GAO-PAO dominated metabolism in both the test reactors 7 and 8.

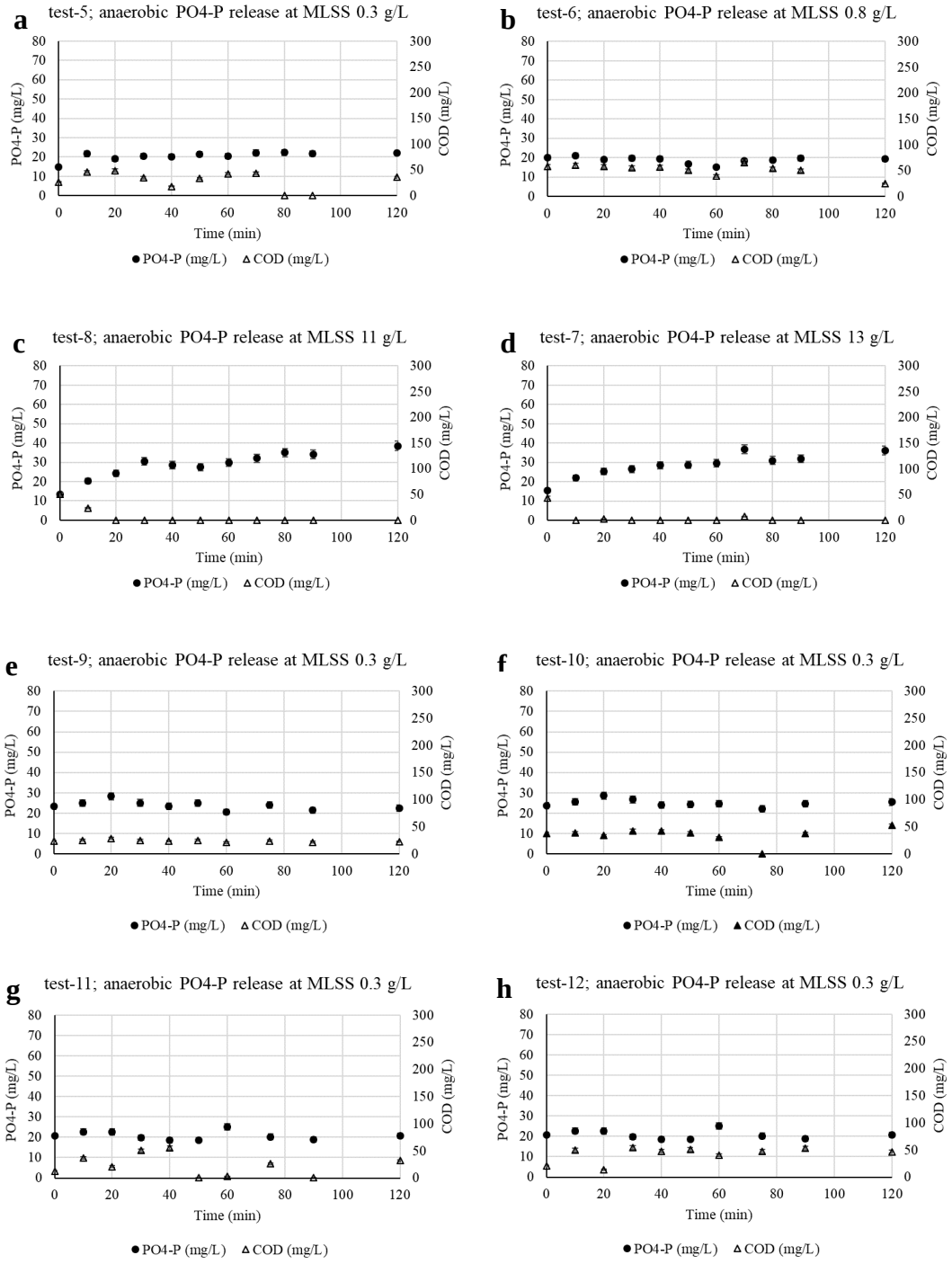

Figure 11. a, b, c, d, e, f, g and h show the trend of anaerobic PO_4^{3-}-P release and COD uptake during the anaerobic period of mixed sludge maintained at different MLSS concentrations

Even if the PO_4^{3-}-P release rate was sometimes higher when performed with low MLSS (0.3 g/L) as in tests 10 and 12, there were cases with no anaerobic PO_4^{3-}-P release when experiments were performed with low MLSS (0.3 g/L) as in the case of test reactors 6, 9, and 11. The COD utilization was also very high in all the cases with low MLSS (in test reactors 6, 9, 11, 10, and 12) therefore the P-release/C up-take ratio was also low (< 0.25 P-mol C-mol^{-1}) in the reactors with very low MLSS, suggesting GAO dominated metabolism.

4.2.2 The effect in sieved granules

The effect of MLSS (low and high MLSS) on granule size 2-4 mm cannot be compared as all the test reactors (test reactors 13, 17, 18, and 20) with 2-4 mm granules were at relatively high MLSS concentration (2.8, 6, 8, and 5 g/L for the test reactors 13, 17, 18, and 20 respectively). The effect of MLSS cannot be compared for granule size > 4mm as well since there was only one test reactor (test reactor 15) with sieved granules of size > 4mm at 0.75 g/L. The kinetic and stoichiometric parameters of interest for all sieved granules have been listed in Table 4. The linear trend of PO_4^{3-}-P release was observed in all the test reactors with granule size 2-4 mm except for test reactor 13 (with MLSS 2.8 g/L). The P-release/C up-take ratio also suggests PAO dominated metabolism in all the test reactors with granules size 2-4 mm and maintained at high MLSS expect for test reactor 13.

Table 4. Kinetic and stoichiometric parameters of tests 13-20 performed with different granule sizes.

Test	Granule size (mm)	MLSS (g/L)	COD consumption (mg COD/ (g MLSS.hour)	PO_4^{3-}-P release (mg P)/ (g MLSS.hour)	P-release/C up-take (P-mol C-mol^{-1})
13	2-4	2.8	-0.4	0.6	-1.7
14	1-2	0.9	3.5	-0.4	-0.1
15	>4	0.8	36.2	4.3	0.1
16	2-1	2.5	4.1	3.2	0.8
17	2-4	6.2	4.5	3.4	0.8
18	2-4	8.3	3.3	1.6	0.5
19	1-2	4.9	5.7	0.1	0.0
20	2-4	5.4	5.1	3.0	0.8

There was no PO_4^{3-}-P activity i.e. neither release nor uptake in the test reactor 14 with granules 1-2 mm (at low MLSS) but with the consumption of 3.5 mg COD g $MLSS^{-1}$ h^{-1} during the anaerobic phase. Denitrification of 1.6 mg NO_3^--N g $MLSS^{-1}$ h^{-1} has taken place for which theoretical COD requirement was calculated as 5.5 mg COD g $MLSS^{-1}$ h^{-1}. Hence, theoretically, all the COD has been utilized for denitrification in the test reactor 14. In the test reactor, 16 (with granules 1-2 mm and high MLSS) the theoretical COD utilized for denitrification was zero, while in the test reactor 19 it was about 25 % of total COD consumption.

Ammonium adsorbed on the surface of the granules even after sludge washing might have oxidized to nitrate during the pre-aeration phase and a small amount of nitrate around 3-5 mg/L as shown in Figure 12 has been observed in test reactors during the anaerobic phase. When low MLSS is maintained, the rate of denitrification was also low. As there was a presence of nitrate and carbon source, maybe denitrification was favoured and would have suppressed the PO_4^{3-}-P release, as the redox conditions were anoxic and similar phenomenon has been observed by Kuba et al., (2014). Meanwhile when the test reactors were maintained at high MLSS, even when nitrate was present (around 5 mg/L), COD utilized for denitrification seems to be lesser when compared to COD available for PO_4^{3-}-P release. Hence, maintaining high MLSS during the test helps in maintaining the test reactors anaerobic as even if small nitrate is present it would be taken up in a short period. Therefore, while performing Bio-P activity test the interference of acetate being taken up for denitrification instead as planned for anaerobic PO_4^{3-}-P release activity in the granules is significantly reduced when MLSS is maintained relatively high.

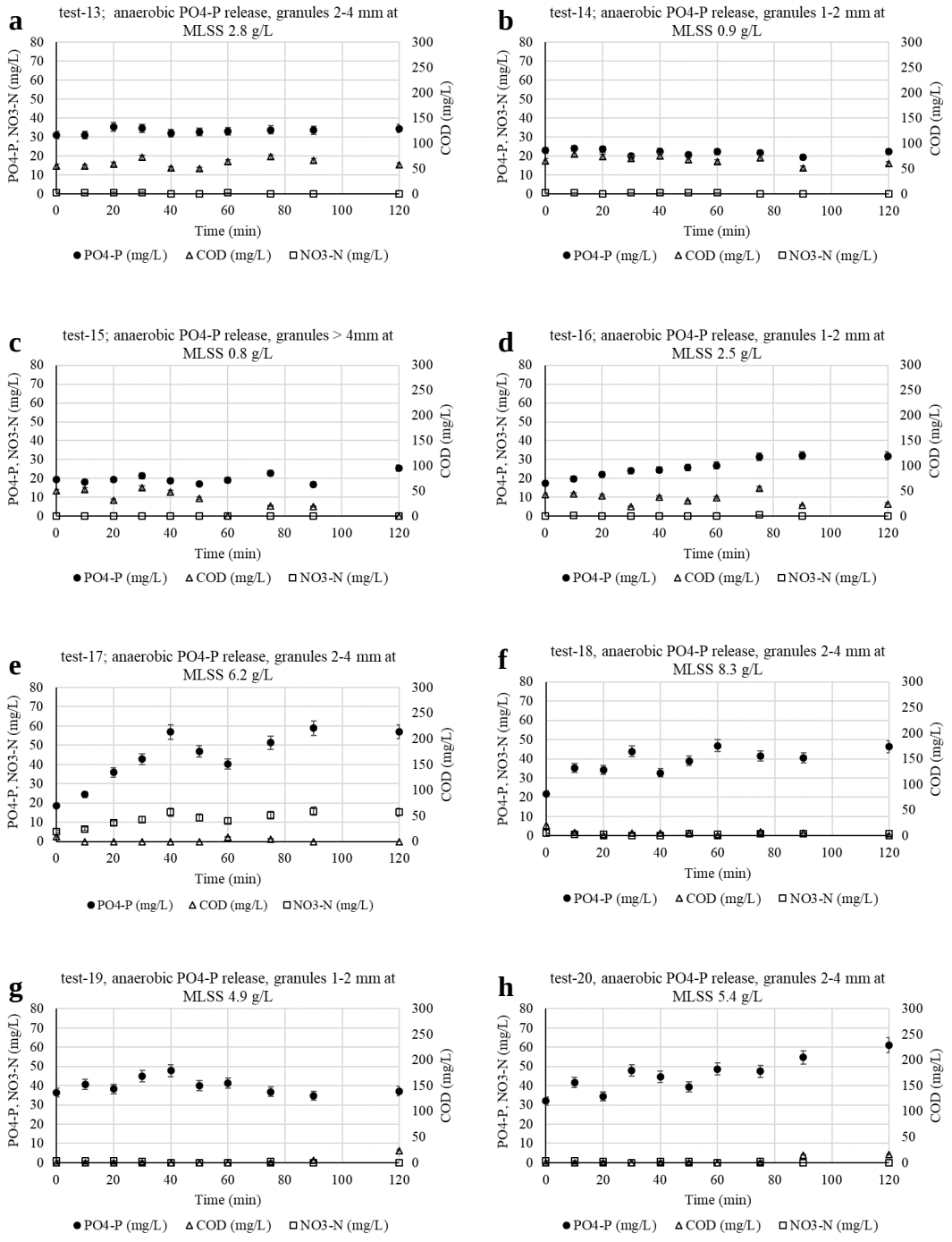

Figure 12. a, b, c, d, e, f, g, and h show the trend of anaerobic PO_4^{3-}-P release and COD uptake during the anaerobic period of sieved granules maintained at different MLSS concentrations.

4.3 Effect of pH on anaerobic PO_4^{3-}-P release kinetics

The maximum anaerobic PO_4^{3-}-P release rate in mixed granules was at 5.3 and 5.2 mg PO_4^{3-}-P g $MLSS^{-1}$ h^{-1}, when pH was maintained at 7.5 for test 21 and test 22 respectively. Meanwhile, the maximum PO_4^{3-}-P release rate at pH 7 was 4.2 and 3.0 mg PO_4^{3-}-P g $MLSS^{-1}$ h^{-1} for test reactors 23 and 24 respectively. Thus, the maximum PO_4^{3-}-P release rate of mixed granules was higher at pH 7.5 in both the tests when compared with the PO_4^{3-}-P release rate for tests maintained at pH 7. The phenomenon of increase in pH favouring the PAO metabolism over GAO's was observed in previous studies in the literature as well (Filipe et al., 2001; Lopez-vazquez et al., 2009; Oehmen et al., 2005). The total mean PO_4^{3-}-P release at pH 7.5 was 84.5 mg PO_4^{3-}-P, while for pH 7 it was 88.5 mg PO_4^{3-}-P. The mean MLSS of tests at pH 7 and 7.5 were 15.5 g L^{-1} and 20 g L^{-1} respectively.

Table 5. Kinetic and stoichiometric parameters for test 21-24.

Test	MLSS (g/L)	P release (mg PO_4^{3-}-P g $MLSS^{-1}$ h^{-1})	COD consumption (mg COD g $MLSS^{-1}$ h^{-1})	P-release/C up-take (P-mol C-mol^{-1})	pH
21	14	5.38	14.98	0.38	7.5
22	17	5.22	11.60	0.50	
23	19	4.29	16.72	0.26	7
24	21	3.09	14.39	0.22	

The mean P-release/C up-take ratio was 0.44 and 0.25 P-mol C-mol^{-1} respectively for anaerobic PO_4^{3-}-P release tests maintained at pH 7.5 and pH 7 respectively. The high P-release/C up-takeratio indicates PAO dominated metabolism when tests were performed at pH 7.5 and GAO dominated metabolism when the tests were performed at pH 7. The results from the tests suggest there might be GAO metabolism in the granules and it might have been suppressed by PAO metabolism at higher pH as observed in the literature (Filipe et al., 2001; Lopez-vazquez et al., 2009; Adrian Oehmen et al., 2005).

The mean PO_4^{3-}-P uptake rate during the pre-aeration phase were 0.33 and 0.54 mg PO_4^{3-}-P g $MLSS^{-1}$ h^{-1} for tests performed at pH 7.5 and pH 7 respectively. In all the four experiments performed, most of the COD was utilized within the first 1-hour form

the start of the test as shown in Figure 13 a, b, c, and d. The maximum PO_4^{3-}-P release rate was also observed within 60 minutes from the start of the anaerobic period. The PO_4^{3-}-P release curves were more flattened in the second hour of the anaerobic phase as there was no acetate available for uptake. The correlation between K and PO_4^{3-}-P release was 0.99, 0.98, 0.97 and 0.97 for tests 21, 22, 23, and 24 respectively. The correlation between PO_4^{3-}-P and Mg release were 0.99, 0.98, 0.99 and 0.99 for tests 21, 22, 23 and 24 respectively. While the correlation between Mg and K release was 0.98, 0.97, 0.97, and 0.97 for tests 21, 22, 23, and 24 respectively and the graphs are shown can be seen in Appendix-F. The strong correlation between cations (Mg and K) and PO_4^{3-}-P release suggests that the release of the ions was from breakage of poly-P reserves to take up acetate during the anaerobic period (Wentzel et al., 2000).

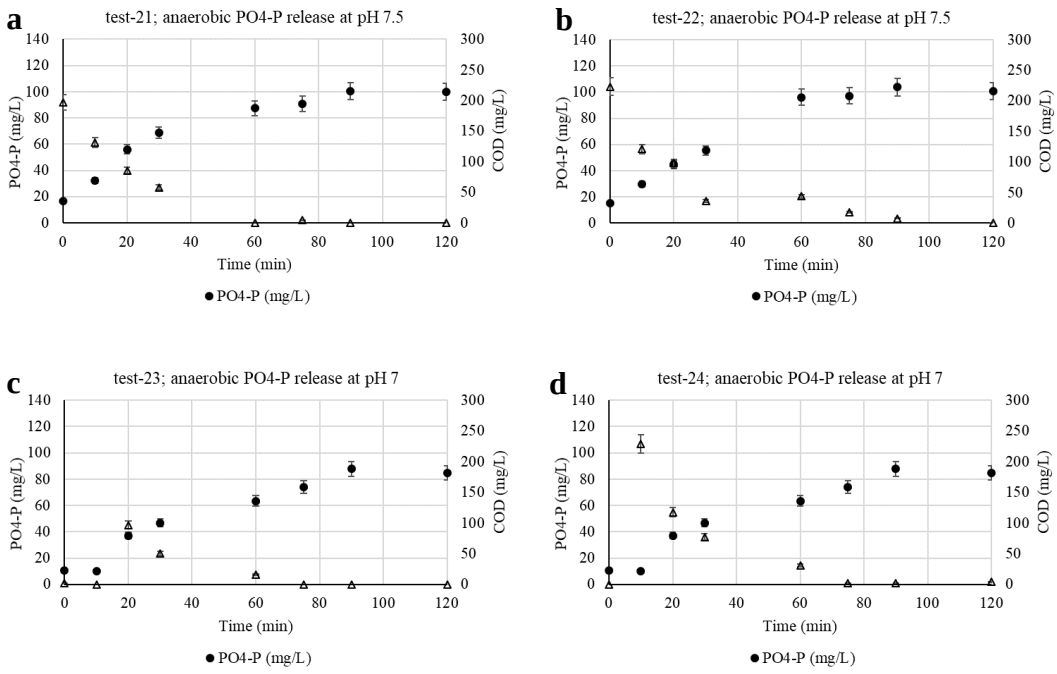

Figure 13. a, b, c, and d show the trend of anaerobic PO_4^{3-}-P release and COD up-take during the anaerobic period of mixed granules maintained at different pH.

4.4 Batch activity test with mixed sludge

4.4.1 Bio-P activity test

The Total Solids (TS) in the test reactors 25 and 26 were 19 and 21 g/L respectively. There was no P-uptake during the pre-aeration phase in test reactor 25, while it was 0.3 mg PO_4^{3-}-P g TS^{-1} h^{-1} in test reactor 26. The PO_4^{3-}-P release rate in the tests 25 and 26 were 1.5 and 1.8 mg PO_4^{3-}-P g TS^{-1} h^{-1} respectively. The P-release/C up-take ratio for test reactors 25 and 26 were 0.5, 0.24 P-mol C-mol^{-1}, suggesting PAO dominated metabolism in test reactor 25 and GAO dominated metabolism in test reactor 26. The PO_4^{3-}-P uptake rate during the aeration phase was 3.3 and 3.8 mg PO_4^{3-}-P g TS^{-1} h^{-1} respectively. The trend of PO_4^{3-}-P release, COD utilization, and PO_4^{3-}-P uptake during the activity test has been illustrated in Figure 14. The P-release/C up-take ratio suggests the presence of GAO metabolism in the granules especially in test reactor 26 (van Loosdrecht et al., 2016).

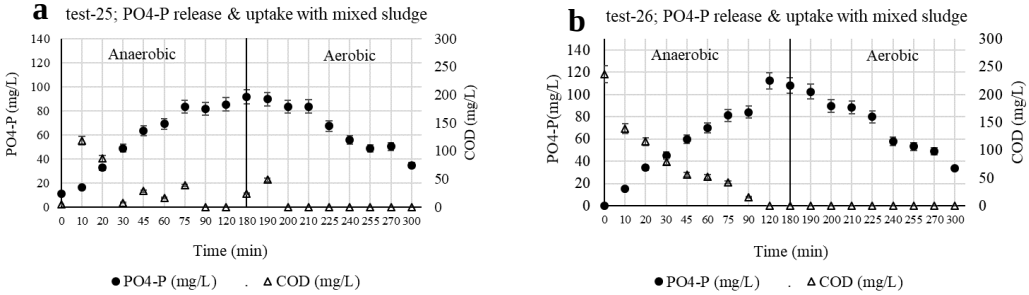

Figure 14. a and b illustrate the trend of PO_4^{3-}-P release and uptake in test mixed granules respectively.

If the PO_4^{3-}-P uptake rate during the pre-aeration phase and the corresponding PO_4^{3-}-P uptake rate during the aerobic phase i.e. after 3 hours of anaerobic phase was observed, it can be noticed that the PO_4^{3-}-P uptake rate has substantially increased (more than 10 times). Figure 15 illustrates the history of the sludge sample before it was transferred to the test reactors. There is a possibility that during the sludge transport and the long storage in the refrigerator for about 16 hours, PAOs in the sludge would have released some PO_4^{3-}-P for anaerobic cell maintenance. In the subsequent sludge washing step, the internally stored PHAs might have oxidized to a considerable extent (van Loosdrecht et al., 2016). Hence, during the pre-aeration phase due to the low availability of internally stored PHAs, PO_4^{3-}-P uptake rate was low. While on the anaerobic phase, the PAOs has taken up acetate and would have formed PHAs, thereby

replenishing it's PHA reserves. Hence, the sludge when exposed to aerobic phase again after the anaerobic phase, it probably had enough PHAs to take up PO_4^{3-}-P and this explains the improved PO_4^{3-}-P uptake rate observed during the aerobic phase after the 3-hour anaerobic phase when compared to the uptake rate during the pre-aeration phase.

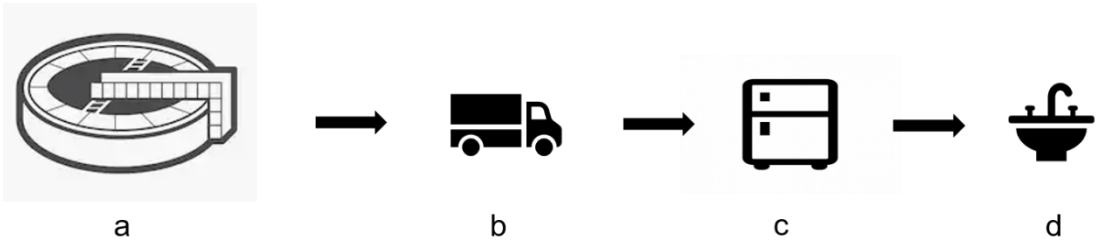

Figure 15. a) sludge samples were taken out from WWTP during aeration phase b) sludge transport in icebox (anaerobic conditions) c) stored in the refrigerator for about 16 hours (anaerobic conditions) d) sludge washing (aerobic conditions) before the test.

4.4.2 Nitrification and denitrification activity test

4.4.2.1 Nitrification batch activity test

The total solids in the test reactors 27 and 28 were 18 and 19 g/L respectively. The mass balance of nitrogen ions during the tests was as shown in Table 6.

Table 6. Mass balance of nitrogen ions for test 27 and 28.

Test	Ammonium oxidation rate (mg NH_4^+-N g TS^{-1} h^{-1})	Nitrite and nitrate production rate (mg NH_4^+-N g TS^{-1} h^{-1})	Ammonium utilized for cell assimilation (mg NH_4^+-N g TS^{-1} h^{-1})	Unaccounted nitrite and nitrate (mg NH_4^+-N g TS^{-1} h^{-1})
27	1.46	0.90	0.01	0.55
28	1.20	1.21	0.00	0.00

There was a 29% less nitrate produced compared to ammonium oxidized in test reactor 27, while there was a 2.5% higher nitrate produced than the ammonium oxidized in test reactor 28 and the values has been calculated using mass balance. Theoretical nitrate utilized for SND (based on mass balance) in the aerobic phase in test reactor 27 was 0.3 mg NO_3^--N g TS^{-1} h^{-1}, which was 24% of the total theoretical nitrate produced. Nitrite ions at the beginning and the end of the test were almost the same with no

accumulation. Simultaneous PO_4^{3-}-P uptake was also observed in addition to nitrification at 0.1 and 0.2 mg PO_4^{3-}-P g TS^{-1} h^{-1}, respectively for test reactors 27 and 28. The trend of ammonium oxidation, nitrate production, and PO_4^{3-}-P uptake has been shown in Figure 16.

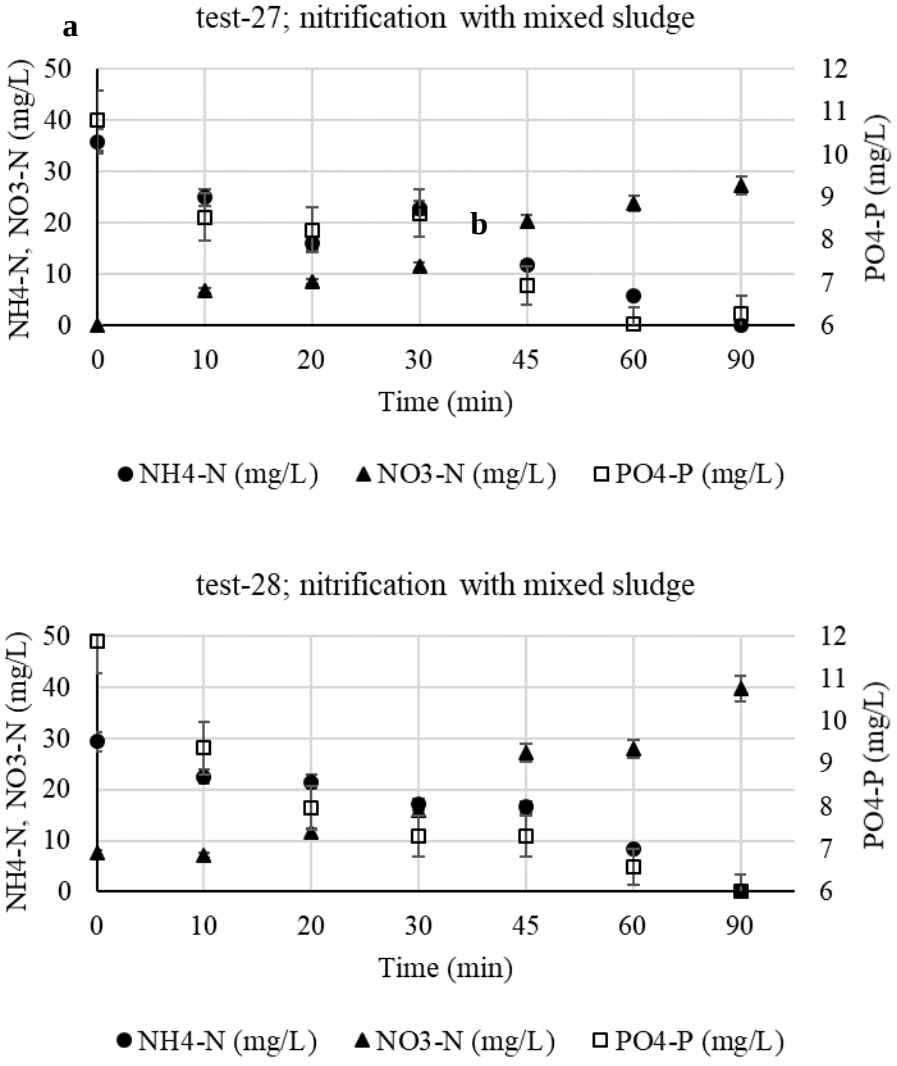

Figure 16. a and b illustrate the trend of NH_4^+-N, PO_4^{3-}-P uptake and NO_3^--N production during nitrification in mixed granules.

The difference in the amount of ammonium oxidized compared to the amount of nitrate produced during the aerobic phase suggests that SND occurred, occurring at different depths of the granules and in compact activated sludge. The PO_4^{3-}-P uptake that took place simultaneously with the nitrification also indicates the SNDP potential of the granules. The reason for the rate of nitrate production being higher than the

ammonium oxidized in test reactor 28 remains unknown and possibly due to some analytical error or else maybe even due to the nitrification of ammonium adsorbed on the surface of the granules. The absence of nitrite accumulation in both the test reactors indicates that there is a balance between two steps involved in nitrification i.e. ammonium oxidation to nitrite by AOB, nitrite oxidation to nitrite oxidation to nitrate by NOB (Oleszkiewicz, 2016).

4.4.2.2 Denitrification batch activity test

The Total Solids of the test reactors were 18 and 19 g/L respectively for test reactors 29 and 30. The denitrification rate was 1.1 and 1.0 mg NO_3^--N g TS^{-1} h^{-1} for test reactors 29 and 30 respectively. The COD utilized during the test period for denitrification was 14 and 11 mg COD g TS^{-1} h^{-1} for test reactors 29 and 30 respectively, which is 28% and 33% of the total COD utilization in the test reactors 1 and 2 respectively. The simultaneous PO_4^{3-}-P release during the denitrification were 1 and 3 mg PO_4^{3-}-P g TS^{-1} h^{-1} for the test reactors 29 and 30 respectively. Thus, the theoretical COD utilization for simultaneous PO_4^{3-}-P release (based on stoichiometry) during the denitrification was 72% and 67% for test reactors 29 and 30 respectively. Figure 17 illustrates the trend of NO_3^--N uptake, acetate uptake, and PO_4^{3-}-P release during denitrification.

The high simultaneous PO_4^{3-}-P release rate during denitrification suggests the potential of the SNDP process occurring in granules. The SNDP potential of the granules has been observed in other tests as well as mentioned in section 4.4.1 of the report. The PO_4^{3-}-P release despite the presence of nitrate was also observed in the literature (Kuba et al., 2014). In the article, the authors observed substantial PO_4^{3-}-P release despite the presence of nitrate, until there was a presence of acetate in the liquid media. They concluded that the presence of nitrate increases the acetate uptake and therefore decreases the P-release/C up-take ratio. In the presence of nitrate, the acetate was utilized for both denitrification and PO_4^{3-}-P release and hence there was a competition between the two microbial guilds in taking up acetate. In this case, even with the presence of nitrate, the PAO seems to outcompete denitrifying guilds for the substrate. The activity of DPAOs (uptake of PO_4^{3-}-P during anoxic condition) seems to have been suppressed. Oehmen and Carvalho (2010) suggested that the requirements to detect and monitor the DPAO PO_4^{3-}-P uptake activity was 1) electron acceptor (NO_3^--N and O_2) and an electron donor (acetate) should not be present in the solution at the same time. 2) Non-limiting source of electron acceptor for PO_4^{3-}-P uptake 3)

availability of enough PHB reserve to uptake PO_4^{3-}-P 4) No nitrite accumulation. Since in our case, both electron acceptor and electron donor were present at the same time and limited availability of electron acceptor (NO_3^--N), there is a possibility that denitrifying ordinary heterotrophs might have outcompeted/supressed the DPAO's PO_4^{3-}-P uptake if there were any.

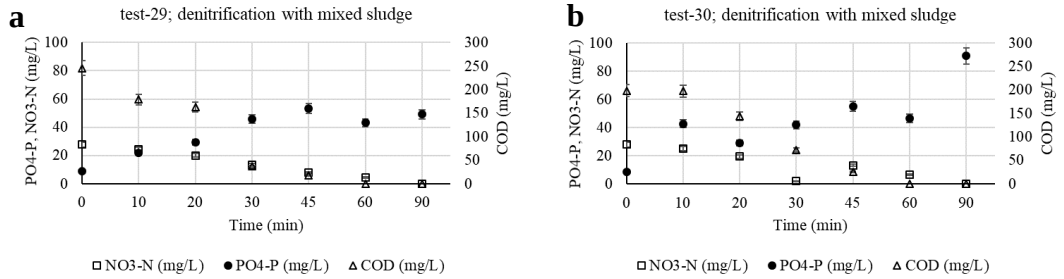

Figure 17. a and b illustrate the trend of NO_3^--N uptake, acetate uptake and PO_4^{3-}-P release during denitrification in mixed granules.

4.5 Effect of granule size

4.5.1 Bio- P activity

Batch activity tests to study the Bio-P activity (anaerobic PO_4^{3-}-P release, PO_4^{3-}-P uptake) in different granule sizes was performed in tests 31-36 and the kinetic and stoichiometric parameters are listed in Table 7 and the trend in the PO_4^{3-}-P ions and COD concentration in the bulk liquid during the test duration has been illustrated in Figure 18.

Table 7. kinetic and stoichiometric parameters of the tests with different granule sizes.

Test	Granule size	MLSS (g/L)	Wastewater	P release (mg PO_4^{3-}-P)/ (g MLSS.hour)	COD consumption (mg COD/ (g MLSS.hour)	P-release/C up-take (P-mol/C-mol)
31	> 2mm	14	synthetic	0.18	2.62	0.09
32	< 2mm	8	synthetic	0.03	4.23	0.01
33	> 2mm	4.8	real	0.75	3.10	0.29
34	< 2mm	3.9	real	0.41	7.25	0.06
35	> 2mm	5.3	synthetic	-0.14	6.45	-0.03
36	< 2mm	4.6	synthetic	0.55	3.58	0.21

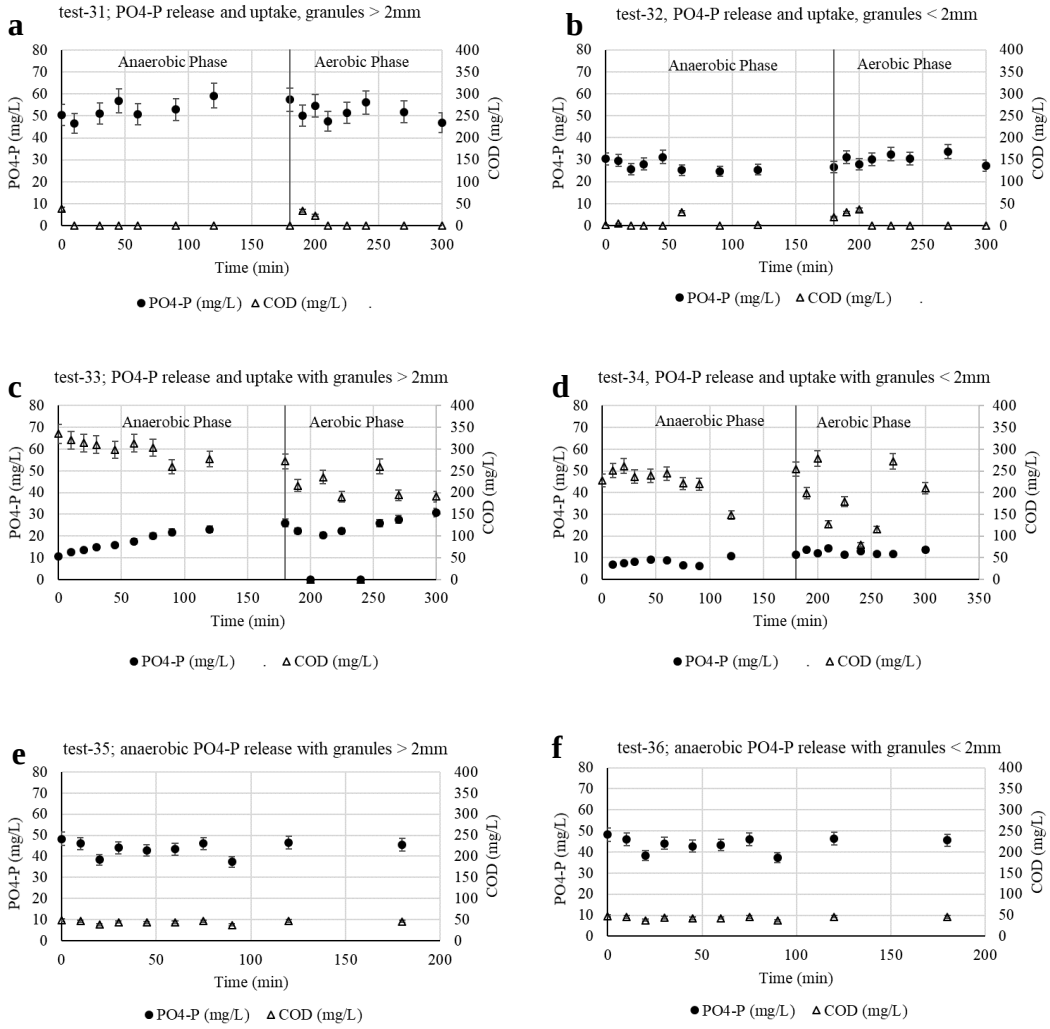

Figure 18. a, b, c, d, e, and f illustrate the trend of PO_4^{3-}-P ions and COD concentration in the bulk liquid during the tests with different granule sizes < 2mm, > 2mm.

The observations on PO_4^{3-}-P release in anaerobic phase from tests 31, 32, 33 and 34 suggest that the PAO activity seems to be higher in larger granules than in the smaller granules, which has also been observed in the literature (Bassin et al., 2012; Tay et al., 2002; Winkler et al., 2011). However, the results from test 35 and 36 show that the PAO activity in smaller granules was higher than in larger granules. No PO_4^{3-}-P release and uptake activity were observed in the large granules in test 35 and the reason remains unknown. The low P-release/C up-take ratio suggests the dominance of GAO metabolism in both the granule sizes. GAO dominance was not expected as the tests 33-36 were performed at high pH of 7.5±0.1. The reason for GAO dominance and PAO metabolism suppression remains to be explored further and can be a result of microbial guilds formed under the environmental conditions in the WWTP. PO_4^{3-}-P

uptake during the aerobic phase in tests 33 and 34 might have been hindered possibly due to competition between PAOs and ordinary heterotrophic organisms (OHO) to take up oxygen, as there was still acetate left in the solution due to carbon leakage as explained in section 2.3.6 of the report. The presence of a high concentration of the acetate in the solution (150 mg/L) might have favoured the OHOs to take up oxygen than the PAOs for PO_4^{3-}-P uptake in tests 33 and 34.

4.5.2 Nitrification in sieved granules

The MLSS concentration of large and small granules during the test was 10 and 6 g/L respectively. The ammonium oxidation rate in large granules was 1.1 mg NH_4^+-N g MLSS^{-1} h^{-1} while for small granules, it has been observed to be 3.2 NH_4^+-N g MLSS^{-1} h^{-1}. The ammonium oxidation rate in small granules was almost 3 times higher than the rate observed in large granules.

While the nitrate produced as a result of nitrification was 0.45 and 0.38 mg NO_3^--N g MLSS^{-1} h^{-1} for large and small granules respectively. Figure 19 a and b show the trend of ammonium oxidation and nitrate production in different granule sizes over the experiment duration. A small P-uptake could be observed in both the granule sizes occurring simultaneously at a rate of 0.32 and 0.21 mg PO_4^{3-}-P g MLSS^{-1} h^{-1} in large and small granules respectively. Figure 19 illustrates the trend of NH_4^+-N, PO_4^{3-}-P uptake and NO_3^--N production during nitrification in different granule sizes. The nitrification rate in smaller granules was almost 3 times higher than in larger granules. The surface area of small granules has been theoretically calculated to be 4 times higher than larger granules (shown in Appendix-A). The PO_4^{3-}-P uptake occurring simultaneously in both the granule sizes reiterates the SNDP potential of the granules as mentioned in section 4.4.2.2 of the report.

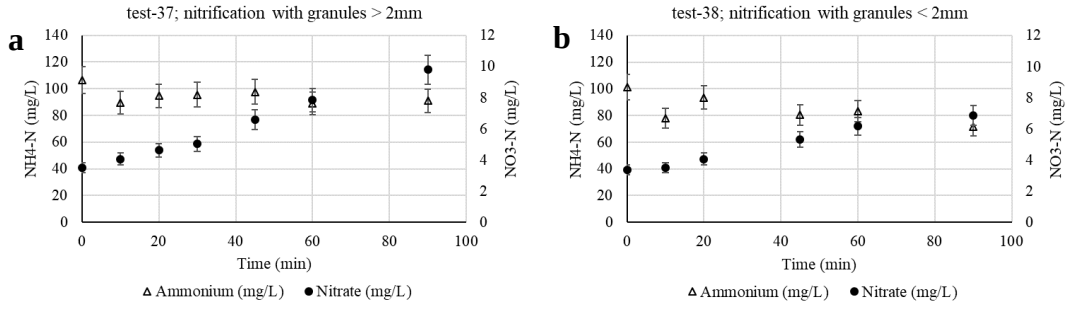

Figure 19. a and b illustrate the trend of NH_4^+-N, PO_4^{3-}-P uptake and NO_3^--N production during nitrification in granule sizes > 2mm, <2mm respectively.

4.5.3 Denitrification in sieved granules

The denitrification rate in small granules was 1.4 times higher than in large granules. The simultaneous P-release rate was two times higher in the larger granules than in the smaller granules as listed in Table 8. The trend of nitrate and COD utilization during the test with large and small granules has been illustrated in Figure 20.

Table 8. kinetics and stoichiometric parameters for denitrification in small and large granules.

Granule size	MLSS (g/L)	Nitrate utilized (NO_3^--N g MLSS^{-1} h^{-1})	COD consumption (mg COD g MLSS^{-1} h^{-1})	Simultaneous P-release (PO_4^{3-}-P g MLSS^{-1} h^{-1})
Large	10	0.38	10.49	0.50
Small	6	0.53	15.84	0.22

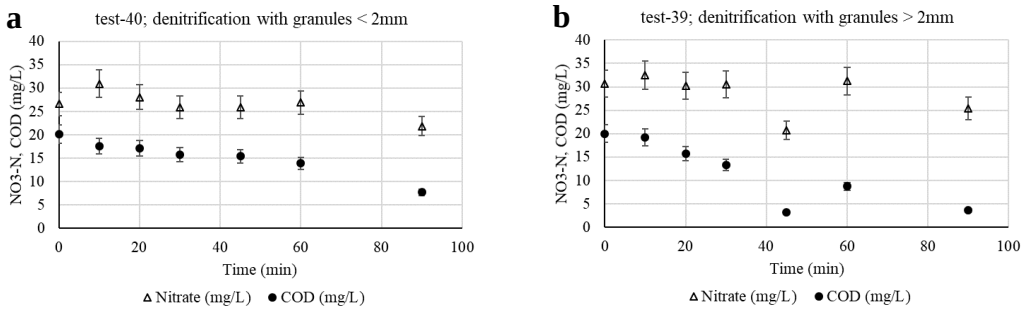

Figure 20. a and b illustrate the trend of NO_3^--N uptake, acetate uptake during denitrification in granule sizes > 2mm, <2mm respectively.

Denitrifying guilds depends on the availability of carbon source and the metabolic end product of nitrification i.e. nitrate for their activity. It has been observed earlier that the nitrification rate was higher in smaller granules than in larger granules. Hence, the denitrifying guilds might be abundant in smaller granules than in larger granules to utilize the nitrate produced from nitrification. Therefore, a higher denitrification rate was observed in smaller granules when compared to larger granules. More tests in the future can help confirm the phenomenon statistically. If the WWTP has problems with nitrogen removal efficiency it can be considered to retain smaller granules in the system as nitrogen removal seems to be better in relatively smaller granules (< 2mm) when compared to larger granules (> 2mm).

5 Conclusions

The major observations from the experiments performed during the batch activity tests performed are as follows:

- Test reactors with high MLSS maintained at pH 7.5±0.1 has been observed to provide optimal environmental conditions to assess the maximum activity of PAO guilds.
- Presence and in some cases dominance of GAO metabolism has been observed irrespective of granule sizes.
- DPAO activity seems to be suppressed or even absent in both granule sizes.
- The strong correlation between simultaneous cation (K and Mg) and PO_4^{3-}-P release indicates the utilization of poly-P release by PAOs to take up acetate during the anaerobic phase.
- Phosphorous removal capacity seems to be higher in relatively larger granules (>2mm), while the nitrogen removal capacity was observed to be faster in smaller granules (< 2mm).

6 Future studies

- Tests with distinct granule sizes to assess Bio-P, Nitrification, and denitrification activity can be performed. For instance, small granules can be between 0.2-1.5 mm and large granules can be > 4mm.
- Tests with enough substrate at the start of the tests must be added so as not to have substrate limiting conditions during the tests, as limited substrate can affect the kinetic parameters.

References

Bassin, J. P., Kleerebezem, R., Dezotti, M., & van Loosdrecht, M. C. M. (2012). Simultaneous nitrogen and phosphate removal in aerobic granular sludge reactors operated at different temperatures. *Water Research*, *46*(12), 3805–3816. https://doi.org/10.1016/j.watres.2012.04.015

Bengtsson, S., de Blois, M., Wilén, B. M., & Gustavsson, D. (2018). Treatment of municipal wastewater with aerobic granular sludge. *Critical Reviews in Environmental Science and Technology*, *48*(2), 119–166. https://doi.org/10.1080/10643389.2018.1439653

Bin, Z., Zhe, C., Zhigang, Q., Min, J., Zhiqiang, C., Zhaoli, C., … Jingfeng, W. (2011). Dynamic and distribution of ammonia-oxidizing bacteria communities during sludge granulation in an anaerobic-aerobic sequencing batch reactor. *Water Research*, *45*(18), 6207–6216. https://doi.org/10.1016/j.watres.2011.09.026

de Kreuk, M. K., Kishida, N., Tsuneda, S., & van Loosdrecht, M. C. M. (2010). Behavior of polymeric substrates in an aerobic granular sludge system. *Water Research*, *44*(20), 5929–5938. https://doi.org/10.1016/j.watres.2010.07.033

De Kreuk, M. K., Van Loosdrecht, M. C. M., & Heijnen, J. J. (2006). *Aerobic granular sludge : scaling up a new technology*. *Department of Biochemical Engineering*.

Derlon, N., Wagner, J., da Costa, R. H. R., & Morgenroth, E. (2016). Formation of aerobic granules for the treatment of real and low-strength municipal wastewater using a sequencing batch reactor operated at constant volume. *Water Research*, *105*, 341–350. https://doi.org/10.1016/j.watres.2016.09.007

Filipe, C. D. M., Daigger, G. T., & Jr, C. P. L. G. (2001). pH as a Key Factor in the Competition Between Glycogen-Accumulating Organisms and Phosphorus-Accumulating Organisms, (April), 223–232.

Henze, M. (1995). *Wastewater treatment: biological and chemical processes*. Springer-Verlag. Retrieved from https://books.google.se/books?id=fBBSAAAAMAAJ

Jabari, P., Yuan, Q., & Oleszkiewicz, J. A. (2016). Potential of hydrolysis of particulate COD in extended anaerobic conditions to enhance biological phosphorous removal. *Biotechnology and Bioengineering*, *113*(11), 2377–2385. https://doi.org/10.1002/bit.25999

Kuba, T., Wachtmeister, A., van Loosdrecht, M., & Heijnen, S. (2014). Effect of nitrate on phosphorus release in biological phosphorus removal systems. *Water Science and Technology*, *30*, 263–269. https://doi.org/10.2166/wst.1994.0277

Layer, M., Adler, A., Reynaert, E., Hernandez, A., Pagni, M., Morgenroth, E., … Derlon, N. (2019). Organic substrate diffusibility governs microbial community composition, nutrient removal performance and kinetics of granulation of aerobic granular sludge. *Water Research X*, *4*, 100033. https://doi.org/10.1016/j.wroa.2019.100033

Li, Y., Liu, Y., Shen, L., & Chen, F. (2008). DO diffusion profile in aerobic granule and its microbiological implications. *Enzyme and Microbial Technology*, *43*(4–5), 349–354. https://doi.org/10.1016/j.enzmictec.2008.04.005

Li, Z. H., Zhu, Y. M., Zhang, Y. L., Zhang, Y. R., He, C. B., & Yang, C. J. (2018). Characterization of aerobic granular sludge of different sizes for nitrogen and phosphorus removal. *Environmental Technology (United Kingdom)*, *0*(0), 1–10. https://doi.org/10.1080/09593330.2018.1483971

Liébana, R. (202). *Microbial Ecology of Granular Sludge Microbial Ecology of Granular Sludge*.

Lochmatter, S., Gonzalez-Gil, G., & Holliger, C. (2013). Optimized aeration strategies for nitrogen and phosphorus removal with aerobic granular sludge. *Water Research*, *47*(16), 6187–6197. https://doi.org/10.1016/j.watres.2013.07.030

Lopez-vazquez, C. M., Oehmen, A., Hooijmans, C. M., Brdjanovic, D., Gijzen, H. J., Yuan, Z., & Loosdrecht, M. C. M. Van. (2009). Modeling the PAO – GAO competition : Effects of carbon source , pH and temperature. *Water Research*, *43*(2), 450–462. https://doi.org/10.1016/j.watres.2008.10.032

Mari, W. (2014). *Magic Granules*. *Igarss 2014*. https://doi.org/10.1007/s13398-014-0173-7.2

Metcalf & Eddy, I., & inc, M. and E. (1979). *Wastewater engineering: treatment, disposal, reuse*. Tata McGraw-Hill. Retrieved from https://books.google.se/books?id=uml3tgEACAAJ

Oehmen, A., Carvalho, G., Lopez-Vazquez, C. M., van Loosdrecht, M. C. M., & Reis, M. A. M. (2010). Incorporating microbial ecology into the metabolic modelling of polyphosphate accumulating organisms and glycogen accumulating organisms. *Water Research*, *44*(17), 4992–5004. https://doi.org/10.1016/j.watres.2010.06.071

Oehmen, Adrian, Lemos, P. C., Carvalho, G., Yuan, Z., Keller, J., Blackall, L. L., & Reis, M. A. M. (2007). Advances in enhanced biological phosphorus removal: From micro to macro scale. *Water Research*, *41*(11), 2271–2300. https://doi.org/10.1016/j.watres.2007.02.030

Oehmen, Adrian, Vives, M. T., Lu, H., & Yuan, Z. (2005). The effect of pH on the competition between polyphosphate- accumulating organisms and glycogen-accumulating organisms, *39*, 3727–3737. https://doi.org/10.1016/j.watres.2005.06.031

Oldham, W. K. (1986). BIOLOGICAL PHOSPHORUS REMOVAL, *20*(12), 1511–1521.

Oleszkiewicz, J. A. (2016). Nitrifying Genera in Activated Sludge May Influence Nitrification Rates, (November). https://doi.org/10.2175/106143007X221373

Pronk, M., de Kreuk, M. K., de Bruin, B., Kamminga, P., Kleerebezem, R., & van Loosdrecht, M. C. M. (2015). Full scale performance of the aerobic granular sludge process for sewage treatment. *Water Research*, *84*, 207–217. https://doi.org/10.1016/j.watres.2015.07.011

Science, W., Dold, P., & Ekama, G. (1985). Kinetics of Biological Phosphorus Release, (November). https://doi.org/10.2166/wst.1985.0221

Science, W., Oehmen, A., & Carvalho, G. (2010). Assessing the abundance and activity of denitrifying polyphosphate accumulating organisms through molecular and chemical techniques molecular and chemical techniques, (April). https://doi.org/10.2166/wst.2010.976

Tay, J., Ivanov, V., Pan, S., & Tay, S. T. (2002). Specific layers in aerobically grown microbial granules, *639798*, 254–257.

van Loosdrecht, M. C. M., Nielsen, P. H., Lopez-Vazquez, C. M., & Brdjanovic, D. (2016, April 1). Experimental Methods in Wastewater Treatment. IWA Publishing. https://doi.org/10.2166/9781780404752

Wagner, J., Weissbrodt, D. G., Manguin, V., Ribeiro da Costa, R. H., Morgenroth, E., & Derlon, N. (2015). Effect of particulate organic substrate on aerobic granulation and operating conditions of sequencing batch reactors. *Water*

Research, *85*, 158–166. https://doi.org/10.1016/j.watres.2015.08.030
Wastewater engineering : treatment and resource recovery. (2014) (Fifth edit). McGraw-Hill Education. Retrieved from http://search.ebscohost.com/login.aspx?direct=true&AuthType=sso&db=cat07470a&AN=clc.07c6f41125e244c2b968445a2b070161&site=eds-live&scope=site&custid=s3911979&authtype=sso&group=main&profile=eds
Wentzel, M., Lotter, L. H., Loewenthal, R. E., & Marais, G. (2000). Metabolic behaviour of Acinetobacter spp . in enhanced biological phosphorus removal - a biochemical model, *12*(4).
Wilén, B. M., Gapes, D., Blackall, L. L., & Keller, J. (2004). Structure and microbial composition of nitrifying microbial aggregates and their relation to internal mass transfer effects. *Water Science and Technology*, *50*(10), 213–220.
Wilén, B. M., Liébana, R., Persson, F., Modin, O., & Hermansson, M. (2018). The mechanisms of granulation of activated sludge in wastewater treatment, its optimization, and impact on effluent quality. *Applied Microbiology and Biotechnology*, *102*(12), 5005–5020. https://doi.org/10.1007/s00253-018-8990-9
Winkler, M., Coats, E. R., & Brinkman, C. K. (2011). Advancing post-anoxic denitrification for biological nutrient removal. *Water Research*, *45*(18), 6119–6130. https://doi.org/10.1016/j.watres.2011.09.006
Winkler, M. K.H., Bassin, J. P., Kleerebezem, R., de Bruin, L. M. M., van den Brand, T. P. H., & Van Loosdrecht, M. C. M. (2011). Selective sludge removal in a segregated aerobic granular biomass system as a strategy to control PAO-GAO competition at high temperatures. *Water Research*, *45*(11), 3291–3299. https://doi.org/10.1016/j.watres.2011.03.024
Winkler, M. K.H., Kleerebezem, R., Strous, M., Chandran, K., & Van Loosdrecht, M. C. M. (2013). Factors influencing the density of aerobic granular sludge. *Applied Microbiology and Biotechnology*, *97*(16), 7459–7468. https://doi.org/10.1007/s00253-012-4459-4
Winkler, Mari K H, Kleerebezem, R., Kuenen, J. G., Yang, J., & Van Loosdrecht, M. C. M. (2011). Segregation of biomass in cyclic anaerobic/aerobic granular sludge allows the enrichment of anaerobic ammonium oxidizing bacteria at low temperatures. *Environmental Science and Technology*, *45*(17), 7330–7337. https://doi.org/10.1021/es201388t
Wu, C. Y., Peng, Y. Z., Wang, S. Y., & Ma, Y. (2010). Enhanced biological phosphorus removal by granular sludge: From macro- to micro-scale. *Water Research*, *44*(3), 807–814. https://doi.org/10.1016/j.watres.2009.10.028
Zheng, Y. M., & Yu, H. Q. (2007). Determination of the pore size distribution and porosity of aerobic granules using size-exclusion chromatography. *Water Research*, *41*(1), 39–46. https://doi.org/10.1016/j.watres.2006.09.015
Zhu, T., Xu, B., & Wu, J. (2018). Experimental and mathematical simulation study on the effect of granule particle size distribution on partial nitrification in aerobic granular reactor. *Biochemical Engineering Journal*, *134*, 22–29. https://doi.org/10.1016/j.bej.2018.03.004

Appendix-A

The theoretical surface area of small and large granules

g_{small} - weight of small granules
g_{large} - weight of large granules
n_{small} - number of small granules
n_{large} - number of large granules
V_{small} - volume of a small granule ($^4/_3\,\pi r_{small}^3$)
V_{large} - volume of a large granule ($^4/_3\,\pi r_{large}^3$)
ρ_{small} - density of small granule
ρ_{large} - density of large granule
r_{small} - radius of small granule
r_{large} - radius of large granule
surface area of an individual small granule = $4\pi r_{small}^2$
surface area of an individual large granule = $4\pi r_{large}^2$

Assumptions

1. Granules are spherical (Mari, 2014)
2. The density of small and large granules are the same, $\rho_{small} = \rho_{large}$
3. The average diameter of large granules is twice the average diameter of small granules
4. Weight of small and large granules taken are same, $g_{small} = g_{large}$

Calculation

$g_{small} = (n_{small}) \times (V_{small}) \times (\rho_{small})$……[5]
$g_{large} = (n_{large}) \times (V_{large}) \times (\rho_{large})$……. [6]
$g_{small} = g_{large}$……equation [3]

as $\rho_{small} = \rho_{large}$ and substituting equation [5] and [6] in equation [7]

$(n_{small}) \times (V_{small}) \times \cancel{(\rho_{small})} = (n_{large}) \times (V_{large}) \times \cancel{(\rho_{large})}$…… [7]
$\Rightarrow n_{small} = (n_{large} \times V_{large})/V_{small}$……equation [8]
$\Rightarrow n_{small} = (n_{large} \times {}^4/_3\,\pi r_{large}^3)/({}^4/_3\,\pi r_{small}^3)$…… [9]

Substituting $r_{small} = x$, $r_{large} = 4x$ in equation 5
$\Rightarrow n_{small} = (n_{large} \times {}^4/_3\,\pi \times 64\,x^3)/({}^4/_3\,\pi \times x^3)$…… [10]
$\Rightarrow n_{small} = 64 \times n_{large}$ ……equation [11]

Total surface area of 'n' small granules = $n_{small} \times 4\pi r_{small}^2$ ……[12]
Total surface area of 'n' large granules = $n_{large} \times 4\pi r_{large}^2$ …… [13]
Substituting $r_{small} = x$, $r_{large} = 4x$ and equation 11 in equation 12
Total specific surface area of 'n' small granules
$= 64 \times n_{large} \times (4\pi r_{large}^2/16)$ ……[14]

⇒ Total surface area of small granules = 4 x total surface area of large granules

Thus, when the average diameter of large granules is twice that of smaller granules and an equal weight of small and large granules are considered, the total surface area of small granules is four times that of the surface area of large granules.

Appendix-B

Data correction for IC results analysis

The steps involved in calculating data correction for IC results and the procedure to convert observed ion concentrations from millimolar to mg/L is illustrated with an example as follows:

Step 1: Fetch IC analysis results and copy it to an Excel File.

Step 2: Table the expected and observed concentration of the standard solution as shown in Table 9.

Table 9. Expected and observed ion concentration (mM) for all the standard ions used

Expected/ observed concentration (mM)	Acetate	PO4-P	NH4-N	NO2-N	NO3-N
0	0	0	0	0	0
0.5	0.6064	0.4391	0.6695	0.4163	0.434
1	1.2847	1.0007	1.3048	0.9647	1.033
1.5	2.0198	1.6304	2.0274	1.5804	1.728

Step 3: Use linear regression function (make sure Data analysis Add on has been installed) in Microsoft Excel to find the slope that fits the observed and expected concentrations of the standard solutions. The summary output from Microsoft Excel for acetate (stated as X variable) is as shown in Figure 21.

SUMMARY OUTPUT

Regression Statistics	
Multiple R	0.9991
R Square	0.9982
Adjusted R Squa	0.9973
Standard Error	0.0338
Observations	4.0000

ANOVA

	df	*SS*	*MS*	*F*	*Significance F*
Regression	1.0000	1.2477	1.2477	1093.2820	0.0009
Residual	2.0000	0.0023	0.0011		
Total	3.0000	1.2500			

	Coefficients	*Standard Error*	*t Stat*	*P-value*	*Lower 95%*	*Upper 95%*	*Lower 95.0%*	*Upper 95.0%*
Intercept	0.0258	0.0277	0.9314	0.4500	-0.0932	0.1448	-0.0932	0.1448
X Variable 1	0.7407	0.0224	33.0648	0.0009	0.6443	0.8371	0.6443	0.8371

Figure 21. Coefficient (slope) for expected and observed concentrations for all the standard ions

Step 4: The slope from step 3 can be used as a **correction factor** that has to be multiplied with observed concentration

Step 5: Convert the concentration from millimolar (mM) to mg/L (the **conversion factor**) based on the molar mass of each ion. Thus, the final ion concentration from IC result analysis is given by equation 15

Final concentration (mg/L) = correction factor x observed concentration (mM) x conversion Factor ……..[15]

Appendix-C

Error bar calculations

Thermo Scientific finnpipette was used for sample preparation for IC analysis. Based on the Thermo Scientific calibration specifications the error due to inaccuracy in transferring liquid volume is listed in Table 10.

Table 10. Inaccuracy levels while handling finpipette for liquid transfers

Pipette	±µL
1 ml finnipipette	6
5 ml finnipipette	25
10 ml finnipipette	50

The standard deviation in dilution factors (maximum and minimum) has been calculated based on the inaccuracy levels as shown in Table 11. The standard error in terms of percentage from Table 11 has been used for including error bars while plotting results for batch activity tests performed.

Table 11. Standard deviation calculation for dilution factors

Performed dilution	Mean Dilution Factor	Max Dilution Factor	Minimum Dilution Factor	Standard Deviation (SD)	SD ± (%)
3.5 times dilution (2 ml sample + 5 ml MilliQ)	3.5	3.54	3.46	0.03	3.23
7 times dilution (1 ml sample + 6 ml MilliQ)	7	7.08	6.92	0.06	6.45
10 times dilution (1 ml sample + 9 ml MilliQ)	10	10.12	9.88	0.09	9.47

Appendix-D

MLSS and MLVSS calculations

The formula for calculation of MLSS and MLVSS is as given in equation 16 and 17.

$$MLSS = \frac{m_s - m_f}{v_{sample}} \text{ g/L} \ldots\ldots\ldots\ldots [16]$$

$$MLVSS = \frac{m_s - m_{s,550}}{v_{sample}} \text{ g/L} \ldots\ldots\ldots\ldots [17]$$

Where,

m_s = mass of filter paper and dried sludge (after placing it in 105^o C) (g)

$m_{s,550}$ = mass of filter paper and dried sludge (after placing it in 550^o C) (g)

m_f = mass of filter paper (g)

V_{sample} = volume of sludge sample (L)

Example calculations

Step 1: Table the m_s, m_f, $m_{s,550}$, V_{sample} and calculate MLSS and MLVSS using the formulas mentioned above as shown in Table 12.

Table 12. MLSS and MLVSS of sludge samples before correction factor

Sample	V_{sample}(ml)	mf (g)	m_s (g)	$m_{s,550}$ (g)	MLSS (g/l)	VSS (g/l)
1	3	0.09	0.0941	0.0892	13.67	16.33
2	3	0.0902	0.0937	0.0893	11.67	14.67
3	3	0.0886	0.093	0.088	14.67	16.67
4	3	0.0888	0.0936	0.0882	16.00	18.00
5	3	0.0878	0.0923	0.0872	15.00	17.00
6	3	0.0891	0.0941	0.0885	16.67	18.67
7	3	0.0897	0.0961	0.0898	21.33	21.00
8	3	0.089	0.0944	0.0882	18.00	20.67
9	3	0.0885	0.0934	0.0881	16.33	17.67
10	3	0.0893	0.0955	0.0892	20.67	21.00
11	3	0.089	0.0947	0.0887	19.00	20.00
12	3	0.0902	0.0961	0.09	19.67	20.33

Step 2: It can be observed that the MLSS value is less than the MLVSS value. Hence the correction factor of 1.004 for m_s (measured m_s x 1.004) and a correction factor of 1.014 for m_f (measured m_f x 1.014) as listed in Table 13.

Table 13. MLSS and MLVSS of sludge samples after correction factor

Sample	Volume(ml)	mf (g)	ms (g)	ms 550 (g)	MLSS (g/l)	VSS (g/l)
1	3	0.09	0.0945	0.0904	14.92	13.43
2	3	0.0902	0.0941	0.0906	12.92	11.75
3	3	0.0886	0.0934	0.0892	15.91	13.80
4	3	0.0888	0.0940	0.0894	17.25	15.13
5	3	0.0878	0.0927	0.0884	16.23	14.16
6	3	0.0891	0.0945	0.0897	17.92	15.79
7	3	0.0897	0.0965	0.0911	22.61	18.09
8	3	0.089	0.0948	0.0894	19.26	17.81
9	3	0.0885	0.0938	0.0893	17.58	14.80
10	3	0.0893	0.0959	0.0904	21.94	18.11
11	3	0.089	0.0951	0.0899	20.26	17.12
12	3	0.0902	0.0965	0.0913	20.95	17.41

It can be observed from Table 13 that after the use of correction factor MLSS value is higher than corresponding MLVSS values indicating the effectiveness of the correction factor used.

Appendix-E

Total Solids and Total Volatile Solids calculations

Step 1: Weigh a dry ceramic cup and note the value as m_c

Step 2: Transfer the crushed granules of known volume (V_{sample}) into the cup using a micropipette

Step 3: Place the cup with the contents in a hot air oven for 24 hours and cool it down in a desiccator until the temperature drops to room temperature

Step 4: Again, weigh the cup and note the value as m_s

Step 5: Place the cup with the contents into a furnace at 550^0C for at least 4 hours, after that cool it down in a desiccator until the temperature drops to room temperature

Step 5: Weigh the cup and note the value as $m_{s,550}$

The formula for Total Solids and Total Volatile Solids is given by equation 17 and 18 respectively

$$\text{Total Solids} = \frac{m_s - m_c}{v_{sample}} \text{ g/L} \quad \text{.....[17]}$$

$$\text{Total Volatile solids} = \frac{m_s - m_{S,550}}{v_{sample}} \text{ g/L} \quad \text{..... [18]}$$

Where,

m_s = mass of cup and dried sludge (after placing it in105^o C oven) (g)

$m_{s,550}$ = mass of cup and dried sludge (after placing it in 550^o C furnace) (g)

m_c = mass of cup (g)

V_{sample} = volume of sludge sample (L)

Appendix-F

The co-release of cations (Mg and K) with P during the anaerobic period for test 21-24 was as shown in Figure 22

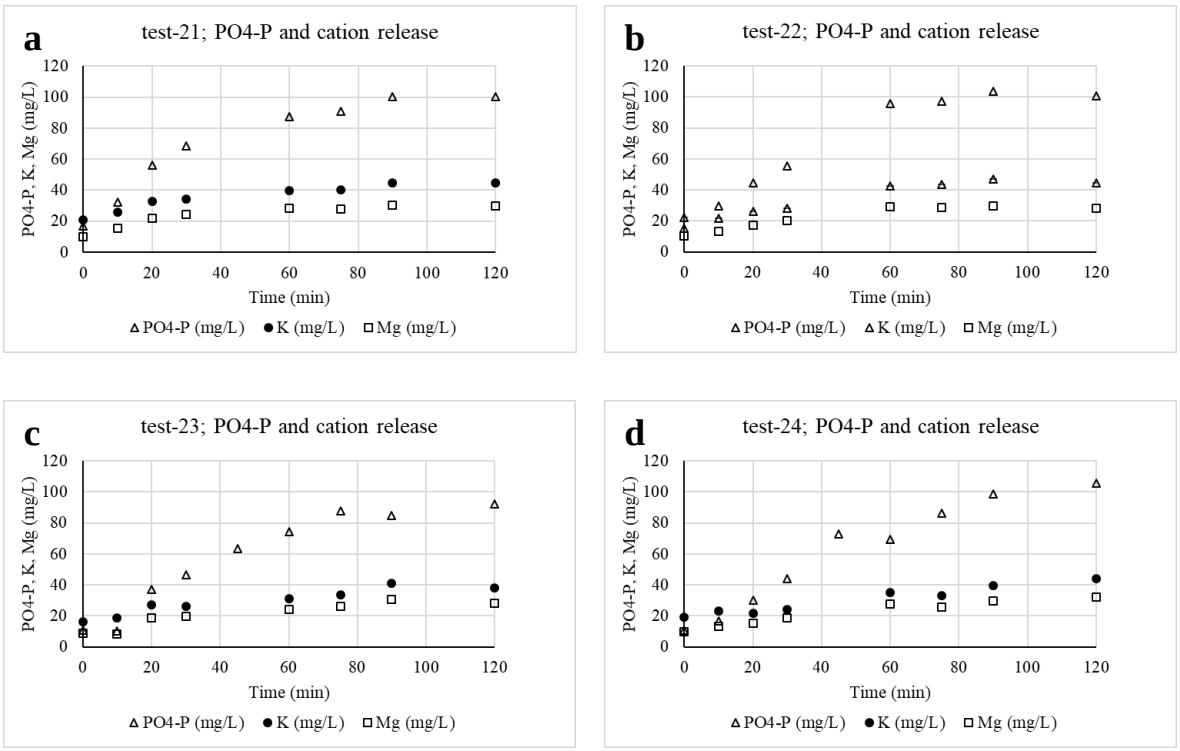

Figure 22. a, b, c, and d illustrate the cations and P release during anaerobic phase in test 21, 22, 23, and 24 respectively.